Paper 4

Meland MY, Dokken TM, Jansen E, Hevrøy K (in preparation) Water mass properties and exchange between the Nordic Seas and the northern North Atlantic during the period 22-6 ka: benthic oxygen isotopic evidence

Water mass properties and exchange between the Nordic Seas and the northern North Atlantic during the period 22-6 ka: benthic oxygen isotopic evidence

Marius Y. Meland[a,b], Trond M. Dokken[a], Eystein Jansen[a,b] and Kjersti Hevrøy[b,c]

[a]*Bjerknes Centre for Climate Research, Allégaten 55, 5007 Bergen, Norway*
[b]*Department of Earth Science, University of Bergen, Allégaten 41, 5007 Bergen, Norway*
[c]*Now at Norsk Hydro ASA, Norway*

Manuscript in preparation

Abstract

Twenty-one glacial ice-volume corrected benthic oxygen isotope records ($\delta^{18}O_{b\text{-}ivc}$) from different water depths in the Nordic Seas and the North Atlantic are compared, supported by ice-volume corrected planktonic oxygen isotopes ($\delta^{18}O_{p\text{-}ivc}$) and benthic carbon isotopes ($\delta^{13}O_b$). During the Last Glacial Maximum (LGM) open-ocean convection produced Glacial North Atlantic Intermediate Water (GNAIW) in the Nordic Seas above 1800 m. GNAIW overflowed the Greenland-Scotland Ridge, and entrained depths above and at least partly below 2000 m in the North Atlantic. Brine formation along the continental margins in the Nordic Seas may have produced deep-water sinking below 1500 m. During the Early Deglaciation (ED) brine-enriched intermediate water masses in the Nordic Seas were formed. These may have overflowed the Greenland-Scotland Ridge, and influenced the North Atlantic water masses down to at least 3700 m. In the Bølling-Allerød (BA) brine formation was reduced, and open-ocean convection was "restarted" in the Nordic Seas. The outflow of this open-ocean convected water, however, was mainly restricted to east of Iceland. A new period of brine formation during the Younger Dryas (YD) is indicated in the water masses at intermediate depths in the Norwegian Sea, but less intensively compared to the ED. There may have been some open-ocean convection and meridional overturning in the Nordic Seas during the YD, giving overflow across the Greenland-Scotland Ridge, but probably reduced compared to the BA. In the Holocene, meridional overturning appears similar to that of today.

Meridional overturning and bottom water overflow from the Nordic Seas to the North Atlantic probably existed more or less continuously, through glacial, deglacial and interglacial times. The mode of overturning was driven by differing proportions of brine-release during sea-ice freezing and open-ocean convection. Even if brine formation is to the most likely explanation of the periodically low $\delta^{18}O_{b\text{-}ivc}$ values in the Nordic Seas, it cannot be excluded that slight temperature increases may also be responsible.

1. Introduction

The Nordic Seas and the Greenland-Scotland Ridge are important areas for ocean circulation. The inflow of warm Atlantic surface/subsurface water into the Nordic Seas, the open-ocean convection in the Nordic Seas, and the returning overflow across the Greenland-Scotland Ridge, form the northern limb of the Atlantic Meridional Overturning Circulation (AMOC). The strength of the AMOC is today reflected in water mass properties, such as temperatures, salinities, and oxygen content, both north and south of the Greenland-Scotland Ridge. The overflow water mass forms the lower part of the North Atlantic Deep Water (NADW) in the North Atlantic. Northwardly advected Atlantic Water brings heat to Northern Europe, and is, in part, responsible for winter air temperatures of the central and eastern Nordic Seas being 10-20˚C higher than the zonal mean (Drange et al. 2005). The strength of the southward bottom water flow across the Greenland-Scotland Ridge may thus indirectly influence the climate of the Nordic Seas and the surrounding landmasses.

In the past, the strength of the AMOC and the rate of water mass exchanges across the Greenland-Scotland Ridge probably changed. These changes should be detectable in the water mass properties at different depths in the Nordic Seas and the North Atlantic. A useful tracer of bottom water mass properties is the $\delta^{18}O_b$ value of benthic foraminifera, as it is controlled by both bottom water temperature and the $\delta^{18}O$ of seawater ($\delta^{18}O_w$) (Shackleton 1974).

Previously published $\delta^{18}O_b$ records in the Nordic Seas and the North Atlantic oscillate between low and high $\delta^{18}O_b$ values during the last glaciation and the last deglaciation. During cold stadial events anomalously low benthic oxygen isotope events are observed (Rasmussen et al. 1996; Vidal et al. 1998; Dokken and Jansen 1999). These events deviate strongly from the global $\delta^{18}O$-ice volume component (Shackleton 1987; Fairbanks 1989; Liu et al. 2004). Some authors suggest that warming of the intermediate and deepwater masses causes these $\delta^{18}O_b$ depletions (Rasmussen et al. 1996; Bauch et al. 2001; Rasmussen and Thomsen 2004),

whereas others suggest that the $\delta^{18}O_b$ depletions are caused by low-$\delta^{18}O$ meltwater in the surface, which then sinks to intermediate and deeper water depths through sea-ice freezing and brine rejection (Vidal et al. 1998; Dokken and Jansen 1999; Labeyrie et al. 2005).

This work aims to study the vertical changes in water mass properties through time inside each of the two basins. These changes imply the type and degree of bottom water mass exchange between these basins. The study compares $\delta^{18}O_b$ records from the North Atlantic and the Nordic Seas (Figure 1a), most of them published, from 800 to 3700 m depth (Figure 1b; Table 1). Thus a useful geographical and vertical coverage in both ocean basins is obtained. Benthic $\delta^{13}C$ and planktonic $\delta^{18}O$ records are used to support the interpretation of the $\delta^{18}O_b$ signals. The work covers the time interval from 22 to 6 ka (see Chronology Section 2.4 for details).

2. Methods and strategy

2.1. Isotope records and bathymetric setting

Twenty-one benthic $\delta^{18}O_b$ records from cores located in the Nordic Seas and the North Atlantic, with depths ranging from 800 to 3700 m (Figures 1a-b, Table 1), were studied. All of the cores display a mean resolution of at least 1000 years: 3 of them have a mean resolution of more than 100 years and 12 of them more than 500 years. The resolution varies between different time intervals of the deglaciation. Most of the $\delta^{18}O_b$ records are previously published (Table 1).

The cores in Figures 1a-b are, for simplicity and overview, divided into 5 groups based on depth and location. Group 1 (G1) consists of cores from intermediate depths (900-1500 m) in the eastern Nordic Seas. Group 2 (G2) are cores from intermediate depths (800-1900 m) in the western Nordic Seas. Group 3 (G3) are cores from depths below 2000 m in the Nordic Seas. Group 4 (G4) includes cores from intermediate depths (1100-1700 m) in the North Atlantic. Group 5 (G5) consists of cores from depths below 2000 m in the North Atlantic. See Figure 1 and Table 1 for an overview and more detailed information.

The Greenland-Scotland Ridge makes a sill, dividing the G1-G3 cores in the Nordic Seas from the G4-G5 cores in the North Atlantic.

2.2. Isotope measurements

The primary evidence will come from $\delta^{18}O_b$ of *Cibicides wuellerstorfi*, *Cibicides lobatulus*, *Cassidulina teretis*, *Melonis barleeanum,* and *Oridorsalis umbonatus*. Planktonic oxygen isotope measurements ($\delta^{18}O_p$) were performed on *Neogloboquadrina pachyderma* sinistral and *Globigerina bulloides* for comparison with the $\delta^{18}O_{b\text{-}ivc}$ measurements in order to interpret similarities and differences in water masses between the surface/subsurface and the bottom water.

The $\delta^{13}C_b$ value of the epibenthic *Cibicides* taxonomic group is regarded as a useful tracer of water mass properties because of its ability to trace $\delta^{13}C$ in bottom water masses (Duplessy et al. 1988; Mackensen et al. 1993; Curry and Oppo 2005). For the other species used, infaunal microhabitats partly exist, and their carbon isotope compositions are, to a varying extent, influenced by the local pore water composition. Therefore, benthic carbon isotopes are not considered for the G1 cores or the HM94-34 core in G3, since the deglacial and glacial intervals are only poorly, or not, covered by $\delta^{13}C_b$ measurements of the *Cibicides* group.

The isotopic data are reported in ‰ versus PDB. $\delta^{18}O_b$ and $\delta^{18}O_{b\text{-}ivc}$ values are reported on the corrected *Uvigerina* scale (+0.64‰ for *Cibicides sp.* and *O. umbonatus*, +0.36‰ for *M. barleeanum*, and +0.00‰ for *C. teretis* (Graham et al. 1981; Jansen et al. 1988)).

In addition, oxygen isotope measurements were also corrected for ice volume:

$$\delta^{18}O_{b\text{-}ivc}\ (‰\ \text{vs. PDB}) = \delta^{18}O_b - \delta^{18}O_{ice\text{-}volume} \quad (1)$$

A similar ice-volume correction was also performed for the planktonic oxygen isotopes ($\delta^{18}O_{p\text{-}ivc}$). The motivation and approach for doing an ice volume correction is described in Section 2.3. Other authors previously performed most of the oxygen isotope measurements, while some are new (see Table 1 for a more detailed information).

2.3. Ice volume correction

It is important to constrain the ice-volume component of the oxygen isotopes ($\delta^{18}O_{ice\text{-}volume}$), since our purpose is to study the combination of bottom temperature and $\delta^{18}O_w$ reflected in the oxygen isotope signal. The $\delta^{18}O_{ice\text{-}volume}$ can be directly tied to the change in global sea level associated with large glaciations (Fairbanks 1989). To calculate $\delta^{18}O_{ice\text{-}volume}$, an ice-volume component of 1.1‰ is used for the LGM. This component is a compromise between the 1.2‰ and 1.0‰ isotope changes suggested by Fairbanks (1989) and Schrag et al. (1996), respectively. A LGM sea level 120 m lower than today is suggested (Fairbanks 1989; Liu et al. 2004). The lowered sea level and ice volume correction is used together with the sea level curve of Liu et al. (2004) (Figure 2) to calculate the ice volume component of the oxygen isotope values for different time intervals of the deglaciation. Assuming that 120 m lowered sea level corresponds to 1.1‰ oxygen isotope increase, gives this formula:

$$\delta^{18}O_{ice\text{-}volume} = \frac{\text{lowered sea level (m)} \times 1.1‰}{120\ \text{m}} \quad (2)$$

2.4 Chronology and age control

The time intervals studied are the Last Glacial Maximum (LGM, 22-19 ka), Early Deglaciation (ED, 19-15 ka), Bølling-Allerød (BA, 15-13 ka), Younger Dryas (YD, 13-11.5 ka), the Early Holocene (EH, 11.5-8 ka) and the Mid Holocene (MH, 8-6 ka). These time definitions may be slightly different from other authors,

but we mean these ages when we refer to a named time interval.

The age control is based on linear interpolation between calendar ages calculated from previously published AMS ^{14}C ages, the Younger Dryas Vedde Ash (Mangerud et al. 1984), and the Early Holocene Saksunarvatn Ash (Mangerud et al. 1986). Age models are produced in previous work. However, all age models are reprocessed here and produced in a consistent manner in this work using the Calib 5.0 software (Stuiver and Reimer 1993). The calendar ages based on AMS ^{14}C ages are calculated using a calculated global reservoir age in Calib 5.0, averaging about 400 years. For the YD a reservoir age of 700 years is used, following Austin et al. (1995). No other reservoir correction has been used, but there may be other reservoir ages for different time intervals and cores. Waelbroeck et al. (2001) suggest a reservoir age of 1900 years for the late ED/early BA in core NA87-22. Hagen (1999) suggests that the bottom water in the Denmark Strait may have a reservoir age of more than 1000 years during the deglaciation, based on data from core JM96-1228. In our study these extended reservoir ages are not used, as there is not yet any consistent dataset available for the various regions and water depths.

During the last deglaciation errors in the age model may give significant errors when calculating the $\delta^{18}O_{b\text{-}ivc}$, since the $\delta^{18}O_{ice\text{-}volume}$ and sea level change significantly and abruptly during the deglaciation. We assume that the $\delta^{18}O_{ice\text{-}volume}$ component and our age models may be regarded as reasonable. During the YD the deposition of the Vedde Ash Layer makes a confident age marker.

In this work, cores containing at least a few AMS ^{14}C ages, the Vedde ash layer, and resolution higher than 500-1000 years were preferred. However, some other cores were also included (Table 1) to obtain sufficient geographical and depth coverage. Figure 3 explains how ages were obtained in these cores. Figure 3 also show all age models used in this study.

2.5 Isotope data and water masses

The benthic oxygen isotope records, both uncorrected and ice-volume-corrected, are shown in Figure 5. $\delta^{13}C_b$ and $\delta^{18}O_p$ records are used to support the interpretation of the $\delta^{18}O_{b\text{-}ivc}$ records. For better comparison between the $\delta^{18}O_{b\text{-}ivc}$ and $\delta^{13}C_b$ records, these records are grouped and shown in Figures 6 and 7. Different water masses are typically characterised by different combinations of $\delta^{13}C_b$ and $\delta^{18}O_{b\text{-}ivc}$ values (Figure 4) (Kroopnick 1980; Oppo and Lehman 1993; Dokken and Jansen 1999). The interpretation of the water masses based on these criteria is not straightforward, and should be read with caution, but they are important for helping the interpretation of $\delta^{18}O_{b\text{-}ivc}$ values.

3. Water mass properties and exchanges - results and paleoceanographic interpretations

3.1. Last Glacial Maximum (LGM, 22-19 ka)

In the Eastern Nordic Seas high $\delta^{18}O_{b\text{-}ivc}$ values (3.9-4.5‰) are observed at depths above 2000 m (Figure 6: G1). In the deeper Nordic Seas (> 2000 m) the $\delta^{18}O_{b\text{-}ivc}$ values are lower (2.7-4.0‰) (Figure 6: G3). We suggest that this difference in $\delta^{18}O_{b\text{-}ivc}$ is caused by larger amounts of brine-rich deepwater being found at depths below 2000 m. Brine formation probably occurred near the continental margins. This interpretation supports investigations by Vorren et al. (1998) and Cofaigh et al. (2004), who suggested that submarine channels, downslope from the continental margins of Greenland, Barents Sea, and northern Norway to > 3000 m depths, were formed by dense water originating from brine formation. These water masses would have been too dense to stabilise at intermediate depths.

Bauch et al. (2001) explain the $\delta^{18}O_b$ depletions of *C. wuellerstorfi* in core PS1243 (Figure 6: G3) as if they represent short intervals of the LGM when water-mass temperatures and food supply resembled more closely an interglacial mode. The $\delta^{18}O_{b\text{-}ivc}$ difference of ~1.5‰ between the LGM and the Holocene (Figure 6) implies a temperature increase of 6˚C compared to Holocene periods (Shackleton 1974), an increase that is difficult to accept at 2700 m depth in the Norwegian Basin, even for short periods. Bauch et al. (2001) argue that the higher and more stable oxygen isotope values of *O. umbonatus* reflect long-term changes, while the $\delta^{18}O_b$ values of *C. wuellerstorfi* show relatively short-lived changes. Based on this argument, our suggestion is that dense brine-enriched water intruded the deeper water masses in the Norwegian Basin, but possibly not continuously. The brine signal may have been diluted by open-ocean convection in between.

Brine-enriched bottom water formed from sea-ice freezing along glacial continental margins are mostly depleted in $\delta^{13}C$, due to the influence from $\delta^{13}C$-depleted glacial meltwater (Dokken and Jansen 1999; Waelbroeck et al. 2006). However, the $\delta^{13}C_b$ values are generally high in the deeper Nordic Seas, averaging 1-1.5‰ (Figure 7: G3), where brine-enriched water is suggested. How can these high values in the brine-enriched deepwater be explained? One explanation is that this deepwater contains signatures of GNAIW, that reflects $\delta^{13}C_b$ values of around 1.5‰ and is formed south of the Greenland-Scotland Ridge (Duplessy et al. 1988; Sarnthein et al. 1994). However, seasonal inflow of AW into the Nordic Seas during the LGM is evident in many records from the Nordic Seas (Veum et al. 1992; Hebbeln et al. 1994; Meland et al. 2005), and it is logical that this inflow has to be balanced by a bottom water outflow in the opposite direction. High epibenthic $\delta^{13}C_b$ values in HM52-43 (Figure 7: G3) are thought to be caused by open-ocean convection (Veum et al. 1992) and high planktonic oxygen isotope values suggest that the central Nordic Seas may have contained high

surface density and potentially suitable conditions for convection (Sarnthein et al. 1995; Meland et al. 2005) To get $\delta^{13}C$ values of 1-1.5‰ in brine-enriched deepwater masses in the central Nordic Seas, water masses with greater $\delta^{13}C$ enrichment should be nearby, possibly as a layer in the intermediate water masses above. Thus, the high $\delta^{13}C_b$ values in the deeper Nordic Seas can be reconciled by open-ocean convection in the central Nordic Seas causing GNAIW to overlie the brine-enriched deepwater.

The lowest $\delta^{18}O_{b\text{-}ivc}$, approaching values below 2‰ in the Nordic Seas are observed in core JM96-1228 at 1079 m in the Denmark Strait (Figure 6: G2). Hagen (1999) suggests that these low values are influenced by foraminifera reworked from the Greenland continental shelf, carrying a light isotopic signal. The location of core JM96-1228 at similar depths as the G1 cores should suggest GNAIW here. Formation of a brine-enriched water mass near Greenland or Iceland, with a similar density to GNAIW, may explain a brine-enriched intermediate water mass in the Denmark Strait. It should also be mentioned that the low $\delta^{18}O_{b\text{-}ivc}$ values correspond to the lowered $\delta^{13}C_b$ values in JM96-1228 (Figures 6 and 7: G2). Therefore we suggest that low $\delta^{18}O_{b\text{-}ivc}$ values are caused by periods of brine formation injected into the intermediate water masses in the western Nordic Seas.

South of the Greenland-Scotland Ridge the $\delta^{18}O_{b\text{-}ivc}$ values are on average 0.4-0.7‰ higher than in the Holocene (Figure 6: G4-G5). This increase corresponds to a temperature decrease of 1.5-3˚C compared with today (Shackleton 1974). The $\delta^{13}C_b$ values are highest in the G4 cores (> 1.4‰, Figure 7), suggesting that these cores are influenced by GNAIW. Below 2000 m in the North Atlantic, a combination of high $\delta^{18}O_{b\text{-}ivc}$ and low $\delta^{13}C_b$ values (Figures 6 and 7: G5) could suggest the influence of Southern Ocean Water (SOW), in agreement with Boyle and Keigwin (1987), Oppo and Lehman (1993) and Curry and Oppo (2005). However, Ninnemann and Charles (2002) showed that LGM $\delta^{13}C_b$ values in the Southern Ocean are on average 1-1.5‰ lower than during the Holocene (Figure 4), at depths below 2000 m. Thus, the lowered $\delta^{13}C_b$ values from the Southern Ocean could be responsible for the low $\delta^{13}C_b$ values at depths corresponding to the modern NADW/SOW boundary (3500-4000 m depth), without higher SOW influence than today. The glacial $\delta^{13}C_b$ values below 2000 m in the North Atlantic are only 0.2-0.7‰ lower than the Holocene values (Figure 7: G5). Based on simple linear mixing relation, we should expect lower $\delta^{13}C$ of waters below 2000 m in the North Atlantic if SOW entrained these depths. Thus, we do not find any clear evidence that SOW entrained water masses from 2000-3000 m in the North Atlantic Ocean. We suggest that the GNAIW formed in the Nordic Seas was able to cross the Greenland-Scotland Ridge, entraining the North Atlantic water masses also below 2000 m, possibly as deep as the modern NADW/SOW boundary. This is in agreement with $^{231}Pa/^{230}Th$ ratios from the deeper North Atlantic (Yu et al. 1996; Gherardi et al. 2005), which give no indication of a shallower SOW during the LGM.

3.2. Early Deglaciation (ED, 19-15 ka)

The strong, 1.5-2‰ depletion of $\delta^{18}O_{b\text{-}ivc}$ at intermediate depths in the southeastern Nordic Seas stands out in the records (Figure 6: G1). It is in approximate synchrony with the massive iceberg release from Laurentide, deposited in the North Atlantic as Heinrich Layer 1 (Heinrich 1988; Bond et al. 1993) starting at 18-18.5 ka and ending at 15-16.5 ka. If temperature alone caused these changes, temperature increases of 6-8˚C into the ED are required (Shackleton 1974), which is highly unlikely. The Barents Sea and Scandinavian ice sheets probably deglaciated considerably at this time, and would have contributed large amounts of melting glacier ice (Elverhøi et al. 1995; Svendsen et al. 1996; Vorren and Laberg 1996). Thus, the cold surface water freshened, potentially making the conditions favourable for sea-ice formation. We believe the $\delta^{18}O_{b\text{-}ivc}$ depletions stem from sea-ice formation and brine rejection to intermediate depths, in agreement with Vidal et al. (1998) and Dokken and Jansen (1999). The good correlation between planktonic and benthic oxygen isotope values (Figure 5: G1) indicates entrainment of brine-enriched water at the eastern margin of the Nordic Seas. The $\delta^{18}O_{b\text{-}ivc}$ depletions are also significant below 2000 m in the Nordic Seas, but of a lower amplitude (Figure 6: G3). Lower, but still high $\delta^{13}C_b$ values were also found in the deep layers (Figure 7: G3). This implies that the brine-rich water mainly filled the intermediate water depths in the Nordic Seas, and only small amounts were sinking deeper. The finding of the large submarine channels downslope from the continental margins support this, since the channels were probably formed by brine rejection (Vorren et al. 1998; Cofaigh et al. 2004). We suggest that the interpreted brine formation is caused by large glacial ice melting starting at 19-18 ka along the Greenland and Barents Sea continental margins, in agreement with Jones and Keigwin (1988), Nam et al. (1995) and Bauch et al. (2001). The timing is consistent with dates reported for the retreat of the Barents Sea ice sheet from the shelf break (Elverhøi et al. 1995; Svendsen et al. 1996; Vorren and Laberg 1996).

In the North Atlantic, a $\delta^{18}O_{b\text{-}ivc}$ decrease is observed, but it is more gradual and fluctuating compared to intermediate depths in the eastern Nordic Seas (Figure 6: G1). This indicates that the Nordic Seas influence the North Atlantic. Another feature is a corresponding, marked $\delta^{13}C_b$ decrease in the ED in the cores above 2200 m (Figure 7: G4 and NA87-22 in G5). We suggest that these lowered $\delta^{13}C_b$ and $\delta^{18}O_{b\text{-}ivc}$ values are due to the influence of meltwater-induced intermediate and deepwater masses from the Nordic Seas, in agreement with Waelbroeck et al. (2006). The Laurentide Ice Sheet, which produced large ice armadas during the ED (deposited as Heinrich Layer 1), may also contribute to this $\delta^{18}O_{b\text{-}ivc}$ depletion. However, since the

most striking $\delta^{18}O_{b\text{-}ivc}$ and $\delta^{13}C_b$ decreases are observed in the easternmost cores in the North Atlantic (Figures 6 and 7), we suggest that a Nordic Seas influence is the most probable.

Below 2500 m in the North Atlantic, the $\delta^{18}O_{b\text{-}ivc}$-depletion corresponds with low $\delta^{13}C_b$ (Figure 7: G5). The $\delta^{13}C_b$ values are, on average, not lowered compared to the LGM. A $\delta^{13}C_b$ increase in the Southern Ocean (Ninnemann and Charles 2002) without any $\delta^{13}C_b$ increase in the North Atlantic (Figure 7: G5) indicates that SOW or brine may be responsible for the low $\delta^{13}C_b$ values. However, the meltwater events identified in Southern Ocean cores are centred around 14 ka, 24 ka, and older ages (Kanfoush et al. 2000), and thus have a different timing to the Heinrich events and the low-$\delta^{18}O_{b\text{-}ivc}$ and $\delta^{13}C_b$ events recorded in the G5 cores. The influence from SOW may thus have no large significance at depths below 2000 m in the North Atlantic. Instead, we suggest that brine-enriched intermediate and deepwater formed in the Nordic Seas did entrain depths below 2500 in the North Atlantic in a significant way.

3.3 Bølling-Allerød (BA, 15-13 ka)

There is an overall tendency for increased $\delta^{18}O_{b\text{-}ivc}$ values in the BA in the Nordic Seas, together with increased $\delta^{13}C_b$ values (Figures 6 and 7: G1-G3). The $\delta^{18}O_{b\text{-}ivc}$ values at intermediate water depths in eastern Nordic Seas (Figure 6: G1) indicate that large meltwater events and brine formation ceased along the European margin.

A marked increase of $\delta^{18}O_{b\text{-}ivc}$ is noted below 2000 m in the Nordic Seas (Figure 6: G3), together with increased $\delta^{13}C_b$ values (Figure 7: G3). We suggest that this combination reflects the transition to a higher degree of open water convection, marking the "turn-on" of open-ocean convection in the Nordic Seas along with a stronger AMOC. This "turn-on" is synchronous with, or possibly slightly leading, a general warming trend and a marked increase in sea level (Figure 2).

In the Iceland Sea, at 1079 m depth, a $\delta^{18}O_{b\text{-}ivc}$ increase is also observed, but the values are fluctuating, and the increase is not obvious overall (Figure 6: JM96-1228 in G2). A similarity between the $\delta^{18}O_{b\text{-}ivc}$ and $\delta^{13}C_b$ changes (Figure 7: JM96-1228 in G2) indicates continuing changes between brine-influenced and convective bottom water in this period. A similar tendency is also seen west of Iceland, at 1683 m (Figure 6: JM96-1225 in G4). Since the isotopic changes are largest in JM96-1228, we suggest that bottom water of a brine-enriched form in periods flowed from the Nordic Seas to the North Atlantic via the Denmark Strait.

In the North Atlantic a similar tendency towards increased $\delta^{18}O_{b\text{-}ivc}$ values is observed (Figure 6: G4-G5). However, the response is delayed and smoothed compared to that in the Nordic Seas (Figure 6: G1-G3). A $\delta^{13}C_b$ increase is, on average, observed in the BA (Figure 7: G4-G5), indicating a larger influence of NADW, but, compared to the Holocene, the average $\delta^{13}C_b$ values in the G5 cores are significantly lower. The $\delta^{13}C_b$ difference between the BA and the Holocene is not so obvious in most of the G2-G4 cores. We propose that NADW with modern characteristics did not entrain depths below 2000 m in the North Atlantic in similar amounts as during the Holocene. SOW or brine-enriched water have probably occupied the majority of the water masses below 2000 m. The observed $\delta^{18}O_{b\text{-}ivc}$ decreases in the North Atlantic may be caused by a combination of warming and a larger influence of brine/SOW, with the latter dominating below 2000 m. A large meltwater pulse from the Antarctica at ~14 ka (Kanfoush et al. 2000) may have caused enhanced brine formation there and promoted transport of brine-enriched SOW entraining depths below 2000 m in the North Atlantic.

Later during the BA (14-13 ka), we suggest that a reduced flow of brine-enriched SOW make the $\delta^{18}O_{b\text{-}ivc}$ values to increase again in the North Atlantic below 2000 m (Figure 6: G5). A temperature decrease may also have occurred, since this period is synchronous with a cooling at the end of the BA. A transition to more NADW-influenced bottom water in the North Atlantic is supported by higher $\delta^{13}C_b$ values than in the ED (Figure 7: G4-G5), and by previous investigations (Boyle and Keigwin 1987; Jansen and Veum 1990; Charles and Fairbanks 1992).

3.4 Younger Dryas (YD, 13-11.5 ka)

The main trend seen during the YD is a decrease in $\delta^{18}O_{b\text{-}ivc}$ (Figure 6). At intermediate depths in the eastern Nordic Seas this decrease is very marked, about ~1‰ (Figure 6: G1). A parallel planktonic isotopic decrease is observed in the three southernmost G1 cores (Figure 5: ENAM93-21, HM79-6/4 and MD99-2284 in G1). The depleted $\delta^{18}O_{b\text{-}ivc}$ values may either be due to brine water influence, or to a warm intermediate water mass from the south (Rasmussen et al. 1996; Rasmussen and Thomsen 2004). If the latter is the case, then the values indicate a temperature increase of 4˚C. We find it unrealistic that an intermediate water mass can be rapidly warmed in this way and still remain dense enough to stay at 1 km or more. Further, we suggest that the parallel planktonic $\delta^{18}O_p$ decreases are due to fresher surface water, not surface warming, particularly as the YD is associated with northern hemisphere cooling.

In the Iceland Sea only core JM96-1228 has a sufficient $\delta^{18}O_{b\text{-}ivc}$ resolution from the G2 records for the YD. A lower and more gradual $\delta^{18}O_{b\text{-}ivc}$ decrease compared to the decrease in the G1 cores is observed here, parallel with a gradual $\delta^{18}O_{p\text{-}ivc}$ decrease (Figure 5: JM96-1228 in G2) and generally high $\delta^{13}C_b$ values (Figure 7: JM96-1228 in G2). Our suggestion is that at least some open-ocean convected water, that was formed somewhere in the Nordic Seas, flowed southwards through the Denmark Strait, with brine formation contributing at least partly to the oxygen isotope signature of the water mass. Decreased $\delta^{18}O_p$

values suggest that brine formation occurred nearby, possibly along the Greenland and/or Iceland margins. Compared to the ED, the $\delta^{18}O_{b\text{-}ivc}$ values are higher overall, suggesting reduced brine formation here compared to the ED. This is supported by the depreciation of turbidity current activity in the submarine channels east of Greenland before the YD (Cofaigh et al. 2004).

We think that brine formation allowed the low-$\delta^{18}O$ meltwater to sink to intermediate depths in the southeastern Nordic Seas, but not to the same extent as during the ED. Cold winters probably abetted the sinking of brine-enriched water along the continental margins, and some open-ocean convection with surface cooling influenced the deepwater formation in the Nordic Seas, giving an enriched $\delta^{13}C$ and slightly diluted $\delta^{18}O_{b\text{-}ivc}$ signal. The brine formation was possibly strongest along the eastern margins in the Nordic Seas, and the brine-enriched water probably did not sink below 2000 m in large amounts, thereby explaining the higher $\delta^{18}O_{b\text{-}ivc}$ values found in the G3 cores (Figure 6). The $\delta^{18}O_{b\text{-}ivc}$ values suggest reduced brine formation during the YD compared to the ED.

The $\delta^{13}C_b$ values in the deeper Nordic Seas are high (Figure 7: G3), indicating formation of at least some convective deepwater, in accordance with Jansen and Veum (1990) and Veum et al. (1992).

At intermediate depths in the North Atlantic $\delta^{18}O_{b\text{-}ivc}$ depletions may be found in the two shallowest cores (Figure 6: G4) and definitely in the southernmost core, JM96-1225, at ~1700 m. This suggests a southwardly outflow of brine-enriched intermediate water through the Denmark Strait.

Below 2000 m in the North Atlantic, there are tendencies towards a weak $\delta^{18}O_{b\text{-}ivc}$ depletion (Figure 6: G5) parallel with an increase in $\delta^{13}C_b$ values (Figure 7: G5). We suggest that the weak $\delta^{18}O_{b\text{-}ivc}$ depletions are diluted forms of the $\delta^{18}O_{b\text{-}ivc}$ signals observed in the Nordic Seas, caused by a flow of brine-enriched intermediate water from the Nordic Seas crossing the Greenland-Scotland Ridge, and mixing with water below 2000 m in the North Atlantic.

If $\delta^{13}C_b$ is regarded as reflecting the strength of ventilation and meridional overturning, the Younger Dryas cold spell cannot easily be explained by an abrupt reduction in the AMOC, in agreement with Jansen and Veum (1990) and Sarnthein et al. (1995). However, south of 40˚N, below 3000 m depth, benthic $\delta^{13}C_b$ values (Boyle and Keigwin 1987; Skinner and Shackleton 2005) and sediment $^{231}Pa/^{230}Th$ ratios (McManus et al. 2004; Gherardi et al. 2005) indicate a reduced NADW flow compared to the Bølling-Allerød and the Holocene. The increased $\delta^{13}C_b$ values that we observed during the YD might not necessarily be a result of a more vigorous AMOC. By not well understood reasons, planktonic $\delta^{13}C$ values of *N. pachyderma* (sin.) increased on average ~0.3‰ from the BA to the YD in the Nordic Seas and the northern North Atlantic (Sarnthein et al. 1995). Our data (Table 1) indicates that $\delta^{13}C$ values of benthic foraminifera increased with only ~0.03‰ on average from the BA to the YD. If open-ocean convection during the YD still was as vigorous as during the BA, one should expect a higher increase in $\delta^{13}C_b$, possibly similar to the planktonic $\delta^{13}C$ increase of ~0.3‰. Thus, we do not think that increased $\delta^{13}C_b$ values are due to an increased strength of the AMOC during the YD. Instead, we suggest that the AMOC was significantly reduced during the YD, and that brine formation contributes more to the slightly weakened $\delta^{18}O_{b\text{-}ivc}$ values in the deeper Nordic Seas and North Atlantic. The $\delta^{13}C_b$ values in the G5 cores (Figure 7) are slightly lower than for the Holocene. This indicates that a SOW-mass partly may have occupied the water column below 2000 m in the North Atlantic, and that NADW flow is reduced compared with today.

3.5. Early and Mid Holocene (EH and MH, 11.5-6 ka)

The start of this time interval is marked by the sudden end of the last glaciation and the transition into the Holocene, where a temperature increase of more than 5˚C is thought to have occurred during approximately 50 years, based on ice cores from Greenland (Grootes et al. 1993).

Higher $\delta^{18}O_{b\text{-}ivc}$ values at the YD-EH transition (11.5-11 ka) are, on average, registered in the Nordic Seas (Figure 6: G1-G3). We suggest that the intermediate and deepwater was less influenced by brine rejection during this transition, because of the warmer climate and reduced sea-ice formation at the continental margins. At the start of the Holocene the deepwater properties resemble more the modern conditions.

A $\delta^{18}O_{b\text{-}ivc}$ and $\delta^{13}C_b$ increase is also observed in the deep North Atlantic cores at the YD-EH transition (Figures 6 and 7: G5), probably attributable to a larger influence of NADW to at least 3700 m depth, and possibly reaching modern characteristics.

Around 11-9 ka, a return to lower $\delta^{18}O_{b\text{-}ivc}$ values is observed mainly in the G1 cores (Figure 6). This decrease is paralleled by SST coolings during Preboreal time (Karpuz and Jansen 1992; Hald and Hagen 1998), which could enhance brine formation. A large meltwater event, caused by the drainage of the Baltic Sea (Hald and Hagen 1998), may contribute significantly to this $\delta^{18}O_{b\text{-}ivc}$ decrease.

After this event, an overall $\delta^{18}O_{b\text{-}ivc}$ increase into the MH in the Nordic Seas cores and partly in the North Atlantic (Figure 6) is observed. The $\delta^{18}O_{b\text{-}ivc}$ values seem also to be higher than during the last 6 ka, even though some authors regard the MH to be warmer than the later parts of the Holocene (Koc et al. 1993; Nesje and Dahl 1993; Andersen et al. 2004). We suggest that the high $\delta^{18}O_{b\text{-}ivc}$ values here are due to decreased brine influence from the Arctic Ocean compared to the Modern (warmer conditions and less sea-ice formation in the Arctic).

The 8.2 ka cold event, found in the $\delta^{18}O$ record from the Greenland ice core GISP2 (Stuiver et al. 1995), does

not stand out in our isotope records, except in the core MD95-2011 at the Vøring plateau (Figure 5: G1). Possibly this is due to low Early Holocene resolution in the other cores, since the extreme part of the record is restricted to a period of about 70 years, interpreted from planktonic oxygen isotopes of MD95-2011 (Risebrobakken et al. 2003).

4. Bottom water overflow across the Greenland-Scotland Ridge: implications for ocean circulation and climate changes

In this section we give a summarized interpretation of the bottom water overflow between the Nordic Seas and the North Atlantic, based on the discussion in Section 3.

During the LGM, high $\delta^{18}O_{b\text{-}ivc}$ and $\delta^{13}C_b$ values (Figures 6-7: G1-G3) suggest a convection cell in the Nordic Seas, allowing intermediate water (GNAIW) in the Nordic Seas to sink to depths above 1500-1800 m. This GNAIW probably flowed southwards across the Greenland-Scotland Ridge, and entrained depths above 2000 m in the North Atlantic, probably explaining the high $\delta^{13}C_b$ values in the G4 cores (Figure 7). This water mass also partly entrained depths down to at least ~3700 m. We do not believe that the deep SOW mass penetrated as shallow (~2000 m) and as far north (~60˚N), as previously suggested by Boyle and Keigwin (1987), Oppo and Lehman (1993) and Curry and Oppo (2005). If it did, it must have been considerably mixed with the GNAIW formed in the Nordic Seas.

During the ED intensive brine formation along the continental margins of the Nordic Seas lead to sinking of brine-enriched water that filled intermediate depths. This suggestion is supported by the $\delta^{18}O_{b\text{-}ivc}$ depletions in the intermediate water cores (Figure 6: G1-G2). Depths below 2000 m were also periodically influenced (Figure 6: G3). The brine-enriched intermediate waters probably crossed the Greenland-Scotland Ridge, and extended southwards into the North Atlantic. Water depths above 2200 m in the North Atlantic were intruded by significant amounts, as reflected by a lowering of $\delta^{18}O_{b\text{-}ivc}$ and $\delta^{13}C_b$ and in the G4 cores and NA87-22 (Figures 6-7). Below 2200 m in the North Atlantic, the combination of periodically low $\delta^{18}O_{b\text{-}ivc}$ and low $\delta^{13}C_b$ values also suggests periodic impulses of brine-enriched water, probably from the Nordic Seas, in agreement with Waelbroeck et al. (2006).

The BA seems to be a period with a circulation system like today, though possibly less vigorous. The combination of high $\delta^{18}O_{b\text{-}ivc}$, $\delta^{13}C_b$ and $\delta^{18}O_p$ values in the Nordic Seas suggest that open-ocean convection may have "restarted" then. A southward outflow of convective overflow water across the Iceland-Scotland Ridge was likely, as indicated by the $\delta^{18}O_{b\text{-}ivc}$ increases in both the North Atlantic and the Nordic Seas, with the increases in the Nordic Seas being greater. The interpreted open-ocean convection in the Nordic Seas may have been important for renewed NADW in the North Atlantic. The outflow of convected water through the Denmark Strait was probably significantly weaker than today. If an outflow existed here, the water was brine-enriched, at least in periods, as shown by the low $\delta^{13}C_b$ and $\delta^{18}O_{b\text{-}ivc}$ values. Probably the NADW was less dominant below 2000 m in the North Atlantic compared with today. Instead, brine-enriched SOW may have more or less occupied the water column, in synchrony with a meltwater event near Antarctica (Kanfoush et al. 2000).

During the YD, some open-ocean convection and meridional overturning in the Nordic Seas may have existed, as supported by high $\delta^{13}C_b$ values in both the Nordic Seas and the North Atlantic (Figure 7). Brine formation along the continental margins in the Nordic Seas supplied the intermediate waters and, partly, waters below 2000 m depths, indicated by $\delta^{18}O_{b\text{-}ivc}$ depletions (Figure 6: G1). In the North Atlantic, $\delta^{18}O_{b\text{-}ivc}$ depletions are partly found in a diluted form (Figure 6: G4-G5), as well as high $\delta^{13}C_b$ values (Figure 7: G4-G5). This combination indicates meridional overturning and southward overflow across the Greenland-Scotland Ridge. However, since a weakened, but still active AMOC is interpreted by others further south in the North Atlantic (McManus et al. 2004; Gherardi et al. 2005), we suggest that open-ocean convection and meridional overturning is reduced in the Nordic Seas, compared to the BA. The high $\delta^{13}C_b$ values were probably caused by some open-ocean convection of surface water enriched in $\delta^{13}C$, the latter deduced from the enhanced $\delta^{13}C$ values of *N. pachyderma* (sin.) in the Nordic Seas and the North Atlantic during the YD (Sarnthein et al. 1995).

In the Holocene, brine formation was likely reduced as indicated by $\delta^{18}O_{b\text{-}ivc}$ increases near the eastern margins in the Nordic Seas (Figure 6: G1). During the period 8-6 ka (MH), the $\delta^{18}O_{b\text{-}ivc}$ values were also higher than today, indicating less brine formation in the Arctic and possibly warmer conditions than for later parts of the Holocene. Slight $\delta^{13}C_b$ and $\delta^{18}O_{b\text{-}ivc}$ increases in the three easternmost G5 cores after the YD-EH transition suggest a more vigorous branch of NADW along the bottom in eastern parts of the North Atlantic (Figures 6-7: G5). Larger amounts of NADW now penetrated the deeper North Atlantic, in agreement with McManus et al. (2004) and Gherardi et al. (2005). Large contributions of this NADW flow probably came from the Nordic Seas.

In summary: Intermediate and deepwater formation through open ocean-convection and/or brine formation may have existed more or less continuously in the Nordic Seas during the time interval 22-6 ka. These mechanisms have given meridional overturning and southward overflow across the Greenland-Scotland Ridge. The strength of the overturning and overflow seems to have varied.

The study implies that cold periods like the ED and the YD cannot entirely be explained by an abrupt reduction in the strength of the AMOC, since our investigations indicate a more or less continuing

meridional overturning. The strength of the AMOC was probably lower during cold periods than today, giving less inflow of warmer surface/subsurface water from the south. If meridional oceanic overturning is responsible for the climate oscillations during the Last Deglaciation, including the rapid shifts to warm conditions, only weak changes in the strength of the AMOC and in the strength of the inflow of Atlantic Water is required to explain large climate oscillations or that more factors are involved.

5. Conclusions

1. During the LGM a well-ventilated intermediate water mass in the Nordic Seas is interpreted, indicated by high $\delta^{18}O_{b\text{-}ivc}$ and $\delta^{13}C_b$ values. This water mass had the characteristics of GNAIW and was layered at depths above 1500-1800 m. It crossed the Greenland-Scotland Ridge and entrained depths in the North Atlantic above 2000 m, and at least partly down to ~3700 m. The GNAIW mass was probably not dense enough to sink further in large amounts in the Nordic Seas, and was more or less replaced by brine-enriched water deeper than 1500 m. Brine formation occurred along the continental margins in the Nordic Seas.

2. During the ED intensive brine formation lead to large-scale sinking of $\delta^{18}O$-depleted meltwater to intermediate depths in the Nordic Seas. The most intensive period for brine formation was during 17-15 ka, in approximate synchrony with the massive iceberg release from Laurentide, deposited in the North Atlantic as Heinrich Layer 1 (Heinrich 1988; Bond et al. 1993). The brine-enriched intermediate water crossed the Greenland-Scotland Ridge and was able to intrude the North Atlantic down to at least ~3700 m.

3. The BA was a period of open-ocean convection in the Nordic Seas, leading to formation of NADW. This water outflowed across the Iceland-Scotland Ridge. The outflow was probably reduced in the Denmark Strait compared with today. If overflow existed in the Denmark Strait, it seems like it was influenced by brine formation along the Greenland and/or Iceland margins. It is uncertain if the NADW during the BA reached deeper than 2000 m in the North Atlantic. If it did, it probably mixed with brine-enriched SOW.

4. The YD is associated with drastic northern hemisphere cooling and seasonality higher than today, implying extreme cold winters. This cooling cannot be entirely explained by a drastic decrease in the strength of the AMOC and the NADW, and is contrary to the high $\delta^{13}C_b$ values. At least some open-ocean convection probably existed in the Nordic Seas. This deep-water mixed with brine-enriched water formed along the margins of the Nordic Seas during the cold winter season. However, enhanced $\delta^{13}C$ values in the surface water in the Nordic Seas and the North Atlantic may explain partly the high $\delta^{13}C_b$ values observed, thus explaining a weaker circulation in the YD compared to the BA and the Holocene. The convected and brine-enriched water flowed southward and crossed the Greenland-Scotland Ridge. Below 2000 m the amounts of NADW was reduced compared with today, in a similar way as during the BA.

5. An overall $\delta^{18}O_{b\text{-}ivc}$ increase at the Younger Dryas-Holocene transition suggests that brine formation ceased in the Nordic Seas. NADW flow became vigorous. The deepwater in the North Atlantic below 2000 m showed increased $\delta^{13}C_b$ values, indicating that the water below 2000 m and to at least ~3700 m had modern characteristics of NADW. Some cores at intermediate depths in the eastern Nordic seas indicate a meltwater event at ~10 ka. This was possibly a meltwater pulse, originating from the last ice melting in Scandinavia, and/or the final drainage of the Baltic Sea.

6. Our conclusion that the marked $\delta^{18}O_{b\text{-}ivc}$ depletions in the Nordic Seas mainly are caused by brine-enriched meltwater seems fairly robust. However, it cannot be excluded that a slight temperature increase can also cause a lowering of the $\delta^{18}O_{b\text{-}ivc}$ values. If other geochemical proxies, for instance benthic foraminiferal Mg/Ca ratios, are able to produce precise temperature estimates in the range of -1 to +5˚C, the temperature component can be sorted out with larger confidence.

7. Other geochemical proxies, like $^{231}Pa/^{230}Th$ in the sediment and Cd/Ca of benthic foraminifera, may help interpretation of the bottom water properties and the strength of the AMOC.

8. Based on our conclusions it seems like that only small changes in the rate of meridional overturning and inflow of Atlantic Water to the Nordic Seas are required to explain the abrupt climate changes that happened during the last deglaciation. Brine formation during cold periods may be a trigger for increasing the net salinity flux to the north by moving warm and high-salinity upper water stored in the subtropical North Atlantic.

Acknowledgements

This manuscript greatly improved by comments and suggestions from Ulysses Silas Ninnemann and Carin Andersson Dahl. Cathy Jenks corrected the English grammar and language. Rune Søraas and Odd Hansen are thanked for keeping the stable isotope mass spectrometer in good shape. This project is funded of the Bjerknes Centre for Climate Research.

References

Andersen C, Koc N, Moros M (2004) A highly unstable Holocene climate in the subpolar North Atlantic: evidence from diatoms. Quaternary Science Reviews 23: 2155-2166

Austin WEN, Bard E, Hunt JB, Kroon D, Peacock JD (1995) The ^{14}C age of the Icelandic Vedde Ash: Implications for Younger Dryas marine reservoir age corrections. Radiocarbon 37: 53-62

Bauch HA, Erlenkeuser H, Spielhagen RF, Struck U, Matthiessen J, Thiede J, Heinemeier J (2001) A multiproxy reconstruction of the evolution of deep and surface water in the subarctic Nordic seas over the last 30,000 yr. Quaternary Science Reviews 20: 659-678

Bond G, Broecker W, Johnsen S, McManus J, Labeyrie L, Jouzel J, Bonani G (1993) Correlations between climate

records from North Atlantic sediments and Greenland ice. Nature 365: 143-147
Boyle EA, Keigwin L (1987) North Atlantic thermohaline circulation during the last 20,000 years: Link to high latitude surface temperature. Nature 330: 35-40
Broecker WS, Andree M, Wolfli W, Oeschger H, Bonani G, Kennett J, Peteet D (1988) The chronology of the last deglaciation: Implications to the cause of the Younger Dryas Event. Paleoceanography 3: 1-19
Charles CD, Fairbanks RG (1992) Evidence from Southern Ocean sediments for the effect of North Atlantic deepwater flux on climate. Nature 355: 416-419
Cofaigh CÓ, Dowdeswell JA, Evans J, Kenyon NH, Taylor J, Mienert J, Wilken M (2004) Timing and significance of glacially influenced mass-wasting in the submarine channels of the Greenland Basin. Marine Geology 207: 39-54
Curry WB, Oppo DW (2005) Glacial water mass geometry and the distribution of $\delta^{13}C$ of ΣCO_2 in the western Atlantic Ocean. Paleoceanography 20: doi:10.1029/2004PA001021
Dokken T, Jansen E (1999) Rapid changes in the mechanism of ocean convection during the last glacial period. Nature 401: 458-461
Drange H, Dokken T, Furevik T, Gerdes R, Berger W, Nesje A, Orvik KA, Skagseth Ø, Skjelvan I, Østerhus S (2005) The Nordic Seas: an overview. In: Drange H, Dokken T, Furevik T, Gerdes R, Berger W (eds) The Nordic Seas: An integrated perspective. AGU Monograph 158, American Geophysical Union, Washington DC, pp 1-10
Duplessy J-C, Labeyrie L, Arnold M, Paterne M, Duprat J, van Weering TCE (1992) Changes in surface salinity of the North Atlantic during the last deglaciation. Nature 358: 485-488
Duplessy J-C, Shackleton NJ, Fairbanks RG, Labeyrie L, Oppo D, Kallel N (1988) Deep water source variations during the last climatic cycle and their impact on the global deepwater circulation. Paleoceanography 3: 343-360
Elverhøi A, Andersen ES, Dokken T, Hebbeln D, Spielhagen RF, Svendsen JI, Sørflaten M, Rørnes A, Hald M, Forsberg CF (1995) The growth and decay of Late Weichselian ice sheet in Western Svalbard and adjacent areas based on provenance studies of marine sediments. Quaternary Research 44: 303-316
Fairbanks RG (1989) A 17,000-year glacio-eustatic sea level record: influence of glacial melting rates on the Younger Dryas event and deep-ocean circulation. Nature 342: 637-642
Gherardi J-M, Labeyrie L, McManus JF, Francois R, Skinner LC, Cortijo E (2005) Evidence from the Northeastern Atlantic basin for variability in the rate of the meridional overturning circulation through the last deglaciation. Earth and Planetary Science Letters 240: 710-723
Graham DW, Corliss BH, Bender ML, Keigwin LD (1981) Carbon and oxygen disequilibria of recent deep-sea benthic foraminifera. Marine Micropaleontology 6: 483-497
Grönvold K, Óskarsson N, Johnsen SJ, Clausen HB, Hammer CU, Bond G, Bard E (1995) Ash layers from Iceland in the Greenland GRIP ice core correlated with oceanic and land sediments. Earth and Planetary Science Letters 135: 149-155
Grootes P, Stuiver M, White JWC, Johnsen S, Jouzel J (1993) Comparison of oxygen isotope records from the GISP2 and Greenland Ice cores. Nature 366: 552-554
Hagen S (1999) North Atlantic paleoceanography and climate history during the last 70 cal. ka. Dr.scient thesis, University of Bergen: 110pp.
Hald M, Hagen S (1998) Early Preboreal cooling in the Nordic seas region triggered by meltwater. Geology 26: 615-618
Hebbeln D, Dokken T, Andersen ES, M. H, Elverhøi A (1994) Moisture supply for northern ice-sheet growth during the Last Glacial Maximum. Nature 370: 357-360
Heinrich H (1988) Origin and consequences of cyclic ice rafting in the northeast Atlantic Ocean during the past 130,000 years. Quaternary Research 29: 142-152
Jansen E, Bleil U, Henrich R, Kringstad L, Slettemark B (1988) Paleoenvironmental changes in the Norwegian Sea and the Northeast Atlantic during the last 2.8 m.y.: Deep Sea Drilling Project/Ocean Drilling Program Sites 610, 642, 643 and 644. Paleoceanography 3: 563-581
Jansen E, Veum T (1990) Evidence for two-step deglaciation and its impact on North Atlantic deep-water circulation. Nature 343: 612-616
Jones GA, Keigwin L (1988) Evidence from Fram Strait (78˚N) for early deglaciation. Nature 336: 56-59
Jung SJA (1996) Wassermassenaustausch zwischen NE-Atlantik und Nordmeer während der letzten 300 000/80 000 Jahre im Abbild stabiler O- und C- Isotope. Berichte aus dem Sonderforschungsbereich 313, University of Kiel, 61, 104 pp.: 104
Kanfoush SL, Hodell DA, Charles CD, Guilderson TP, Mortyn PG, Ninnemann US (2000) Millennial-scale instability of the Antarctic ice sheet during the last glaciation. Science 288: 1815-1818
Karpuz NK, Jansen E (1992) A high-resolution diatom record of the last deglaciation from the SE Norwegian Sea: documentation of rapid climatic changes. Paleoceanography 7: 499-520
Koc N, Jansen E, Haflidason H (1993) Paleoceanographic reconstructions of surface ocean conditions in the Greenland, Iceland and Norwegian seas through the last 14 ka based on diatoms. Quaternary Science Reviews 12: 115-140
Kroopnick P (1980) The distribution of $\delta^{13}C$ in the Atlantic Ocean. Earth and Planetary Science Letters 49: 469-484
Labeyrie L, Waelbroeck C, Cortijo E, Michel E, Duplessy J-C (2005) Changes in deep water hydrology during the Last Deglaciation. Comptes Rendus Geoscience 337: 919-927
Liu JP, Milliman JD, Gao S, Cheng P (2004) Holocene development of the Yellow River´s subaqueous delta. Marine Geology 209: 45-67
Mackensen A, Hubberten HW, Bickert T, Fischer G, Fütterer DK (1993) The $\delta^{13}C$ in benthic foraminiferal tests of *Fontbotia wuellerstorfi* (Schwager) relative to the $\delta^{13}C$ of dissolved inorganic carbon in Southern Ocean deep water: implications for glacial ocean circulation models. Paleoceanography 8: 587-610
Mangerud J, Furnes H, Johansen J (1986) A 9000-year old ash bed on the Faroe Islands. Quaternary Research 26: 262-265
Mangerud J, Lie SE, Furnes H, Kristiansen IL, Lømo L (1984) A Younger Dryas ash bed in western Norway, and its possible correlations with tephra in cores from the Norwegian sea and the North Atlantic. Quaternary Research 21: 85-104
Manighetti B, McCave IN (1995) Late glacial and Holocene palaeocurrents around Rockall Bank, NE Atlantic Ocean. Paleoceanography 10: 611-626
Maslin M (1992) A study of the paleoceanography of the N.E. Atlantic in the late Pleistocene. PhD thesis. Department of Earth Sciences, Cambridge, England

McManus JF, Francois R, Gherardi J-M, Keigwin LD, Brown-Leger S (2004) Collapse and rapid resumption of Atlantic meridional circulation linked to deglacial climate changes. Nature 428: 834-837

Meland MY, Jansen E, Elderfield H (2005) Constraints on SST estimates for the northern North Atlantic/Nordic Seas during the LGM. Quaternary Science Reviews 24: 835-852

Nam S-I, Ruediger S, Grobe H, Hubberten H (1995) Late Quaternary glacial-interglacial changes in sediment composition at the East Greenland continental margin and their paleoceanographic implications. Marine Geology 122: 243-262

Nesje A, Dahl SO (1993) Lateglacial and Holocene glacier fluctuations and climate variations in western Norway: A review. Quaternary Science Reviews 12: 255-261

Ninnemann US, Charles CD (2002) Changes in the mode of Southern Ocean circulation over the last glacial cycle revealed by foraminiferal stable isotopic variability. Earth and Planetary Science Letters 201: 383-396

Oppo DW, Lehman SJ (1993) Mid-depth circulation of the subpolar North Atlantic during the Last Glacial Maximum. Science 259

Oppo DW, Lehman SJ (1995) Suborbital timescale variability of North Atlantic Deep Water during the past 200,000 years. Paleoceanography 10: 901-910

Rasmussen T, Thomsen E, van Weering TCE (1998) Cyclic sedimentation on the Faeroe Drift 53-10 ka BP related to climatic variations. In: Stoker MS, Evans D, Cramp A (eds) Geological processes on continental margins: sedimentation, mass-wasting and stability. Geological Society, London, pp 255-267

Rasmussen TL, Thomsen E (2004) The role of the North Atlantic Drift in the millennial timescale glacial climate fluctuations. Palaeogeography Palaeoclimatology Palaeoecology 210: 101-116

Rasmussen TL, Thomsen E, van Weering TCE, Labeyrie L (1996) Rapid changes in surface and deep water conditions at the Faeroe Margin during the last 58,000 years. Paleoceanography 11: 757-771

Risebrobakken B, Jansen E, Andersson C, Mjelde E, Hevrøy K (2003) A high-resolution study of Holocene paleoclimatic and paleoceanographic changes in the Nordic Seas. Paleoceanography 18: doi:10.1029/2002PA000764

Sarnthein M, Jansen E, Weinelt M, Arnold M, Duplessy J-C, Erlenkeuser H, Flatøy A, Johannessen G, Johannessen T, Jung SJA, Koc N, Labeyrie L, Maslin M, Pflaumann U, Schulz H (1995) Variations in Atlantic surface ocean paleoceanography, 50°-80°N: A time-slice record of the last 30,000 years. Paleoceanography 10: 1063-1094

Sarnthein M, Stattegger K, Dreger D, Erlenkeuser H, Grootes PM, Haupt BJ, Jung SJA, Kiefer T, Kuhnt W, Pflaumann U, Schäfer-Neth C, Schulz H, Schulz M, Seidov D, Simstich J, van Kreveld S, Vogelsang E, Völker A, Weinelt M (2000) Fundamental modes and abrupt changes in North Atlantic circulation and climate over the last 60 ky – concepts, reconstruction and numerical modelling. In: Schäfer P, Ritzrau W, Schlüter M, Thiede J (eds) The northern North Atlantic: a changing environment. Springer, Berlin, pp 365-410

Sarnthein M, Winn K, Jung SJA, Duplessy J-C, Labeyrie L, Erlenkeuser H, Ganssen G (1994) Changes in east Atlantic deepwater circulation over the last 30,000 years: Eight time slice reconstructions. Paleoceanography 9: 209-267

Schrag DP, Hampt G, Murray DW (1996) Pore fluid constraints on the temperature and oxygen isotopic composition of the glacial ocean. Science 272: 637-642

Shackleton NJ (1974) Attainment of isotopic equilibrium between ocean water and the benthonic foraminifera genus *Uvigerina*: isotopic changes in the ocean during the Last Glacial. Colloques Internationaux du C.N.R.S. 219: 203-209

Shackleton NJ (1987) Oxygen isotopes, ice volume and sea level. Quaternary Science Reviews 6: 183-190

Skinner LC, Shackleton NJ (2005) An Atlantic lead over Pacific deep-water change across Termination I: implications for the application of the marine isotope stage stratigraphy. Quaternary Science Reviews 24: 571-580

Stuiver M, Grootes PM, Braziunas TF (1995) The GISP2 $\delta^{18}O$ climate record of the past 16,500 years, and the role of the Sun, ocean and volcanoes. Quaternary Research 44: 341-354

Stuiver M, Reimer PJ (1993) Extended ^{14}C data base and revised CALIB 3.0 ^{14}C age calibration program. Radiocarbon 35: 215-230

Svendsen JI, Elverhøi A, Mangerud J (1996) The retreat of the Barents Sea Ice Sheet on the western Svalbard margin. Boreas 25: 244-256

Veum T, Jansen E, Arnold M, Beyer I, Duplessy J-C (1992) Water Mass Exchange between the North Atlantic and the Norwegian Sea during the last 28,000 years. Nature 356: 783-785

Vidal L, Labeyrie L, van Weering TCE (1998) Benthic $\delta^{18}O$ records in the North Atlantic over the last glacial period (60-10 kyr): Evidence for brine formation. Paleoceanography 13: 245-251

Voelker AH (1999) Zur Deutung der Dansgaard-Oeschger Ereignisse in ultra-hochauflösenden Sedimentprofilen aus dem Europäischen Nordmeer. PhD thesis, University of Kiel, Germany, 180 pp.

Vogelsang E (1990) Paläo-Ozeanographie des Europäischen Nordmeeres an Hand stabiler Kohlenstoff- und Sauerstoffisotope. PhD thesis, University of Kiel, Germany, 136 pp

Vorren TO, Laberg JS (1996) Late glacial air temperature, oceanographic and ice sheet interactions in the southern Barents Sea region. In: Andrews JT, Austin WEN, Bergsten H, Jennings A (eds) Late Quaternary Palaeoceanography of the North Atlantic Margins. Geological Society Special Publication, pp 303-321

Vorren TO, Laberg JS, Blaume F, Dowdeswell JA, Kenyon NH, Mienert J, Rumohr J, Werner F (1998) The Norwegian-Greenland Sea continental margins: morphology and Late Quaternary sedimentary processes and environment. Quaternary Science Reviews 17: 273-302

Waelbroeck C, Duplessy J-C, Michel E, Labeyrie L, Paillard D, Duprat J (2001) The timing of the last deglaciation in North Atlantic climate records. Nature 412: 724-727

Waelbroeck C, Levi C, Duplessy J-C, Labeyrie L, Michel E, Cortijo E, Bassinot F, Guichard F (2006) Distant origin of circulation changes in the Indian Ocean during the last deglaciation. Earth and Planetary Science Letters 243: 244-251

Yu E-F, Francois R, Bacon MP (1996) Similar rates of modern and last-glacial ocean thermohaline circulation inferred from radiochemical data. Nature 379: 689-694

Table 1
Core positions, water depths, bottom temperatures, salinities, sources of stable isotope records, and sources of radiocarbon measurements and ash layers.
See text in Section 2.1 for information about the group belongings.

Core	Group	Lon.	Lat.	Water depth (m)	T_{bottom} (˚C) JAS	S_{bottom} (˚C) JAS	Reference benthic isotopes	Reference planktic isotopes	Benthic species measured	Planktic species measured	Laboratory source $\delta^{18}O$, $\delta^{13}C$	Reference AMS ^{14}C	Vedde Ash identified by:	Saksunar Ash identified by:	Time interval studied
HM79-6/4	G1	2.55	63.10	900	-0.6	34.91	1	1	CT	NPS	UOB	13	13	13	6-17 ka
ENAM93-21	G1	-4.00	62.74	1020	-0.7	34.91	18	18	MB	NPS	GIF	17	17	17	8-22 ka
MD95-2011	G1	7.64	66.97	1048	-0.4	34.91	19	19	CT	NPS	UOB	19	8	n.i.	6-14 ka
MD95-2010	G1	4.56	66.68	1226	-0.4	34.91	6	6	CT	NPS	UOB	6	6	n.i.	10-22 ka
MD99-2284	G1	-0.98	62.37	1500	-0.9	34.92	5	5	CT	NPS	UOB	5	5	n.i.	6-22 ka
PS2644	G2	-21.77	67.87	778	-0.6	34.91	22	24	CL	NPS	UOK	24	24	n.i.	10-22 ka
JM96-1228	G2	-26.10	67.03	1079	-0.8	34.92	9	9	CL	NPS	UOB	9	9	n.i.	10-22 ka
HM80-60	G2	-11.86	68.90	1869	-0.9	34.91	1	21	CW	NPS	UOB	n.d.	21	n.i.	6-22 ka
M23062	G3	0.10	68.43	2286	-0.9	34.92	25	25	CW	NPS	UOK	25	n.i.	n.i.	6-21 ka
PS1243	G3	-6.55	69.37	2711	-0.9	34.91	2	2	CW/OU	NPS	UOK	2	2	n.i.	6-22 ka
HM52-43	G3	0.73	64.26	2781	-1.0	34.91	23	23	CW	NPS	UOB	23	23	n.i.	6-22 ka
HM94-34	G3	-2.54	73.77	3004	-1.1	34.91	1	21	CW/OU	NPS	UOB	21	21	n.i.	6-22 ka
BOFS17K	G4	-16.50	58.00	1150	5.2	35.07	15	15	CW	NPS/GB	GL	n.d.	n.i.	n.i.	6-22 ka
M23419	G4	-19.74	54.97	1491	3.9	34.96	12	12	CW	NPS/GB	UOK	n.d.	n.i.	n.i.	8-22 ka
JM96-1225	G4	-29.29	64.91	1683	3.6	34.96	9	10	CW	NPS	UOB	9	10	n.i.	8-22 ka
NA87-22	G5	-14.57	55.50	2161	3.5	34.91	20	7	CW	NPS	GIF	7, 26	n.i.	n.i.	6-22 ka
M17051	G5	-31.98	56.17	2300	3.1	34.97	12	12	CW	NPS	UOK	12	n.i.	n.i.	6-22 ka
V23-81	G5	-16.14	54.03	2393	3.1	34.91	11	11	CW	NPS	UOB	3, 4	11	n.i.	6-22 ka
V29-202	G5	-21.00	60.00	2658	3.0	34.96	16	16	CW	GB	WOOD	16	n.i.	n.i.	6-22 ka
M17049	G5	-26.73	55.28	3331	2.9	34.97	12	12	CW	NPS	UOK	12	12	n.i.	6-22 ka
M17045	G5	-16.65	52.43	3663	2.9	34.96	12	12	CW	NPS	UOK	12	12	n.i.	6-22 ka

Notes on Table 1:

1: this work, 2: Bauch et al. (2001), 3: Bond et al. (1993), 4: Broecker et al. (1988), 5: Dokken (unpublished data), 6: Dokken and Jansen (1999), 7: Duplessy et al. (1992), 8: Grønvold et al. (1995), 9: Hagen (1999), 10: Hagen and Hald (2002), 11: Jansen and Veum (1990), 12: Jung (1996), 13: Karpuz and Jansen (1992), 14: Manighetti et al. (1995), 15: Maslin (1992), 16: Oppo and Lehman (1995), 17: Rasmussen et al. (1996), 18: Rasmussen et al. (1998), 19: Risebrobakken et al. (2003), 20: Sarnthein et al. (1994), 21: Sarnthein et al (1995), 22: Sarnthein et al. (1999), 23: Veum et al. (1992), 24: Voelker (1999), 25: Vogelsang (1990), 26: Waelbroeck et al. (2001).

GL = Godwin Laboratory, Cambridge, GIF = Laboratoire mixte CNRS-CEA, Gif sur Yvette, UOB = University of Bergen, UOK = University of Kiel, WOOD = Woods Hole Oceanographic Institution

N.d. = not dated, n.i. = not identified.

Foram. species: CL = *C. lobatulus,* CT = *C. teretis*, CW = *C. wuellerstorfi*, GB = *G. bulloides*, MB = *M. barleeanum*, NPS = *N. pachyderma* (sin.), OU = *O. umbonatu*s

Figure captions

Figure 1. a) Map of the Nordic Seas and the northern North Atlantic with ocean currents and fronts. The studied cores are shown as red circles. b) Bathymetry of the Nordic Seas and the northern North Atlantic. The studied cores are shown as white circles.

Figure 2. Stepwise postglacial sea-level rise, after Liu et al. (2004). The left Y-axis denotes the lowered sea level compared to the Modern. The right Y-axis denotes the inferred global ice-volume component of $\delta^{18}O$ compared to the Modern, calculated from Equation 2 in text.

Figure 3. Age models for all cores, reconstructed in this study. The symbols of calendar ages reflect the calculated ages, based on published AMS ^{14}C datings (see Table 1 for references). The minimum calendar ages point to the lower end of the 1 sigma range, calculated using Calib 5.0 (Stuiver and Reimer 1993), and the maximum calendar ages point to the higher end of the 1 sigma range. The cores HM80-60, BOFS17K and M23419 do not contain AMS ^{14}C datings. HM80-60 is correlated to HM94-34 in the Nordic Seas and the other cores to BOFS5K in the North Atlantic, using planktonic oxygen isotopes. The symbols for age in these three cores therefore points to correlation points. The numbers G1-G5 refer to the group definition described in Section 2.1 and Table 1. The numbers to the right of the core numbers refer to the respective water depths in meters.

Figure 4. Typical $\delta^{18}O_{b\text{-}ivc}$ and $\delta^{13}C_b$ values for epibenthic foraminifera with respect to different water masses. The horizontal and vertical lines mark the approximate ranges for each of the water masses. The $\delta^{18}O_{b\text{-}ivc}$ values are corrected for +0.64‰ (Graham et al. 1981; Jansen et al. 1988). Abbreviations: GNAIW = Glacial North Atlantic Intermediate Water, NADW = North Atlantic Deep Water, NSDW = Norwegian Sea Deep Water, SOW = Southern Ocean Water, LGM = Last Glacial Maximum. The water masses NADW, NSDW and SOW_{modern} represent modern conditions, while the other water masses represent glacial conditions. The ranges should be considered as approximate with reference to isotope data from Vogelsang (1990), Dokken and Jansen (1999), Hagen and Hald (2002), Curry and Oppo (2005) and this work. The question marks mean that the $\delta^{13}C_b$ ranges for brine-enriched water is not well known yet.

Figure 5. $\delta^{18}O$ and $\delta^{13}C_b$ records of planktonic and benthic foraminifera from the cores shown in Figure 1. The records in the right panels are ice-volume corrected using Equation 1 in text. The calendar age scales are deduced from the core depths using the age models of Figure 3. Single vertical black lines in the left panels denote the Vedde Ash Layer (Mangerud et al. 1984), and double vertical black lines denote the Saksunarvatn Ash Layer (Mangerud et al. 1986). The triangles in top of each plot on the left side denote the positions of AMS ^{14}C ages from Figure 3. Horizontal grey lines in the right panels denote the average of $\delta^{18}O_{b\text{-}ivc}$ records covering the 'Modern' (0-6 ka), as long as data from this time interval exist. The vertical lines in the right panels denote the boundaries between the different time intervals. The headers (Group 1-5) denote the "group belonging" of the different cores, with reference to Section 2.1 and Table 1. See Section 2.4 for details about the abbreviations of the time intervals. The cores HM80-60, BOFS17K and M23419 do not contain AMS ^{14}C datings. HM80-60 is correlated to HM94-34 in the Nordic Seas and the other cores to BOFS5K in the North Atlantic, using planktonic oxygen isotopes.

Figure 6. Ice-volume corrected benthic oxygen isotope records. The curves are the same as the benthic oxygen isotope curves in the right panels of Figure 5. The records are grouped based on the group definition described in Section 2.1 and Table 1. Abbreviations: CW = *C. wuellerstorfi*, OU = *O. umbonatus*. See Section 2.4 for details about the time interval abbreviations.

Figure 7. Benthic carbon isotope records. The curves are the same as the benthic carbon isotope curves of Figure 5. The records are grouped based on the group definition described in Section 2.1 and Table 1. See Section 2.4 for details about the time interval abbreviations. Due to the lack of epibenthic $\delta^{13}C_b$ records in the G1 cores, these records are not shown here.

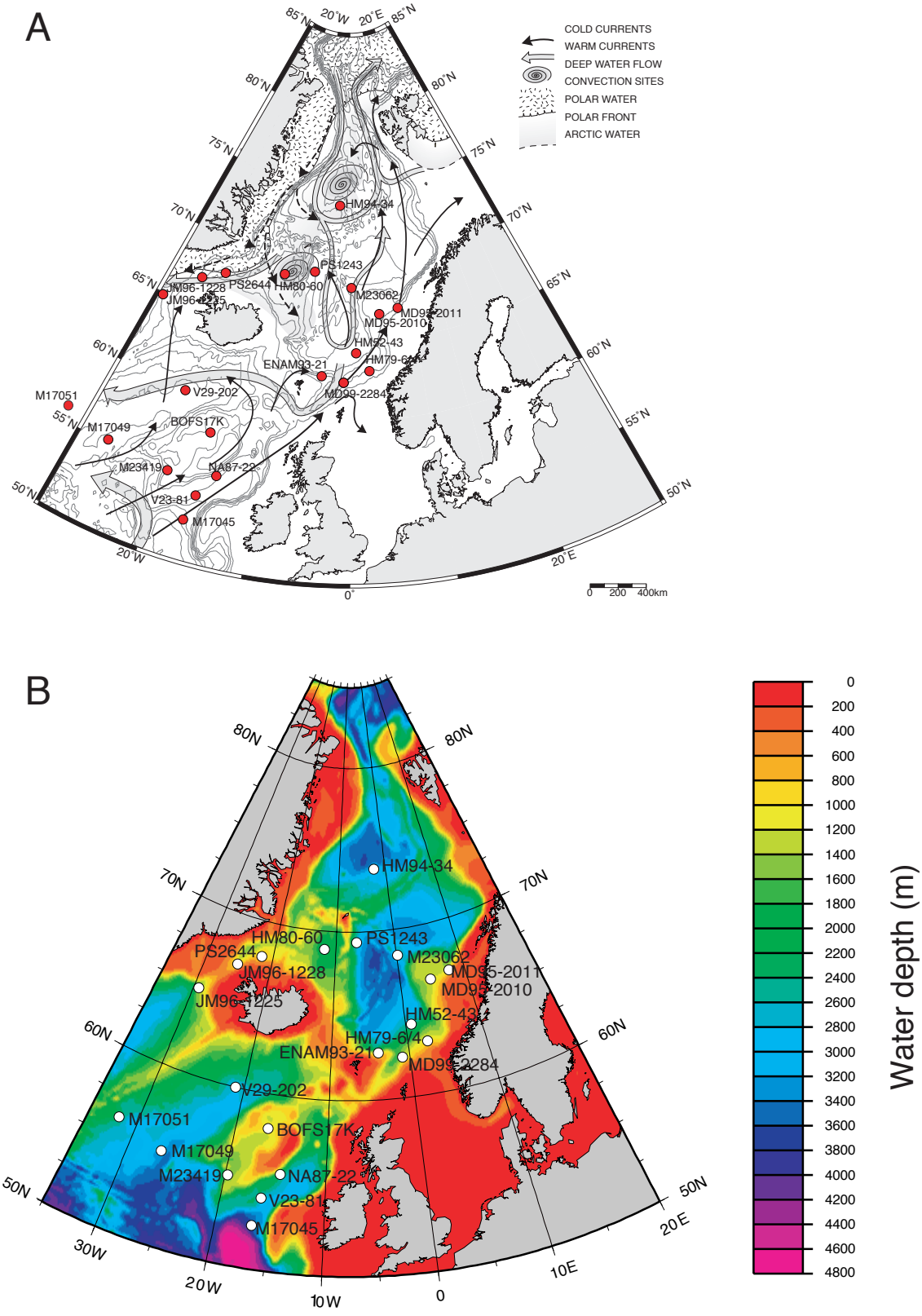
A
COLD CURRENTS
WARM CURRENTS
DEEP WATER FLOW
CONVECTION SITES
POLAR WATER
POLAR FRONT
ARCTIC WATER
HM94-34
PS1243
JM96-1228
PS2644
HM80-60
JM96-1225
M23062
MD95-2011
MD95-2010
HM52-43
HM79-6/4
ENAM93-21
MD99-2284
V29-202
M17051
M17049
BOFS17K
M23419
NA87-22
V23-81
M17045
0 200 400km
B
Water depth (m)
0
200
400
600
800
1000
1200
1400
1600
1800
2000
2200
2400
2600
2800
3000
3200
3400
3600
3800
4000
4200
4400
4600
4800

Figure 1

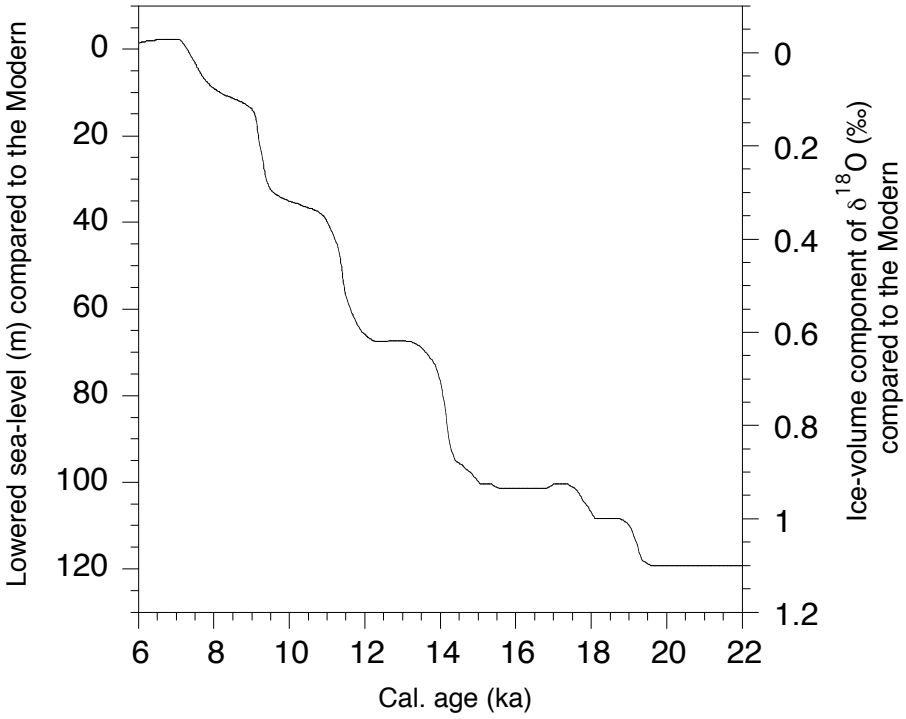
Lowered sea-level (m) compared to the Modern
0
20
40
60
80
100
120
6
8
10
12
14
16
18
20
22
Cal. age (ka)
0
0.2
0.4
0.6
0.8
1
1.2
Ice-volume component of δ18O (‰)
compared to the Modern

Figure 2

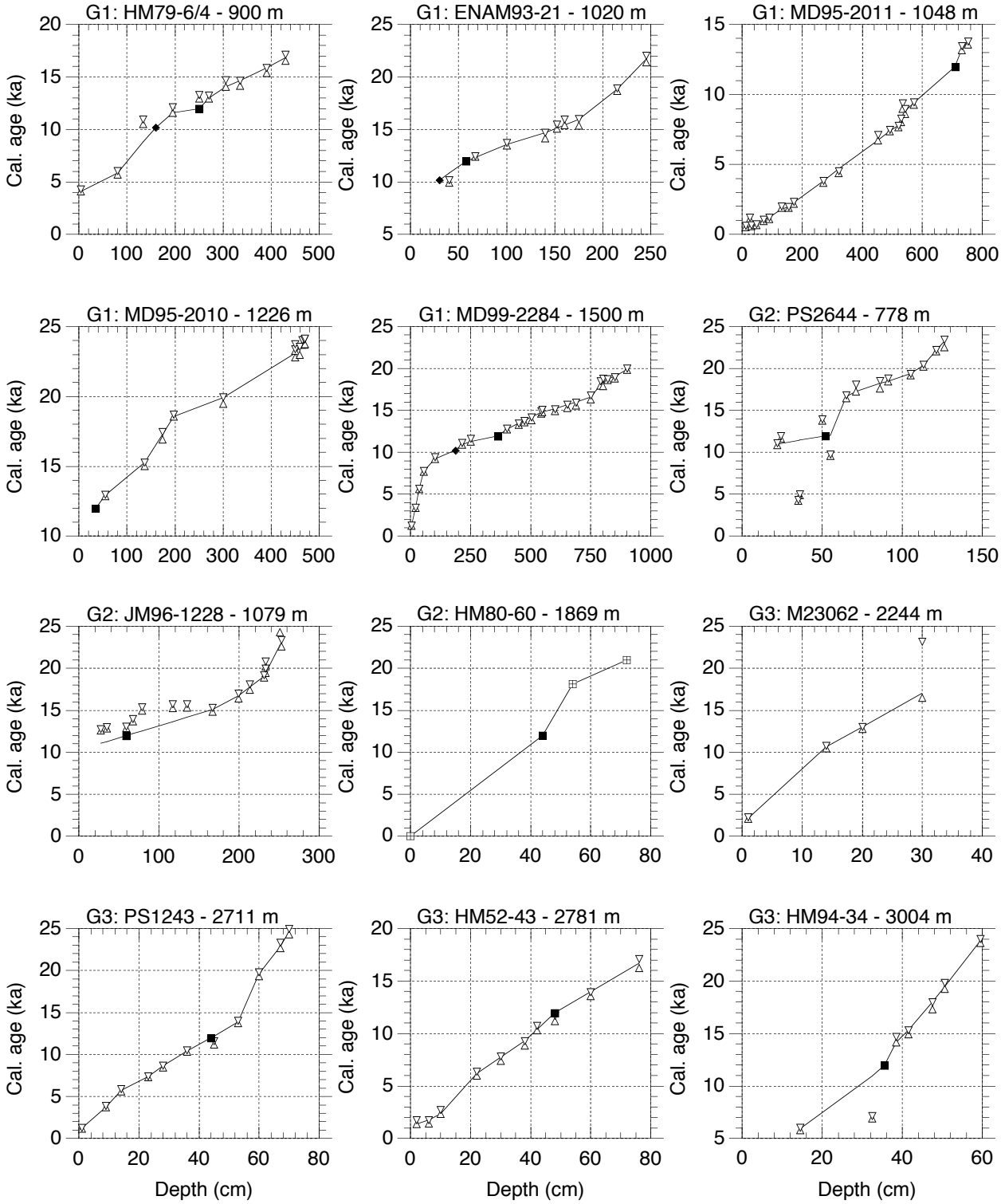

Figure 3 - page 1

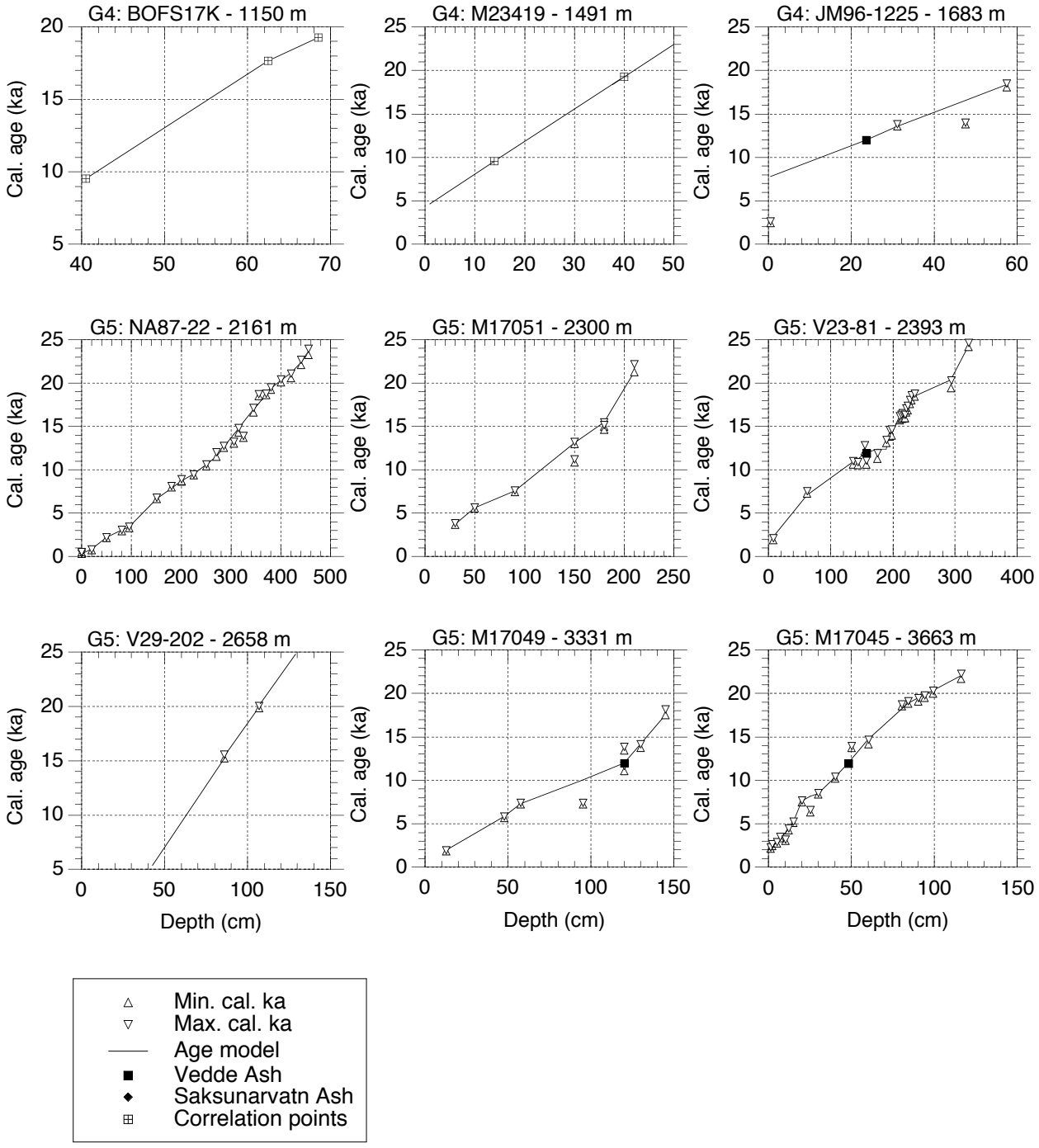

Figure 3 - page 2

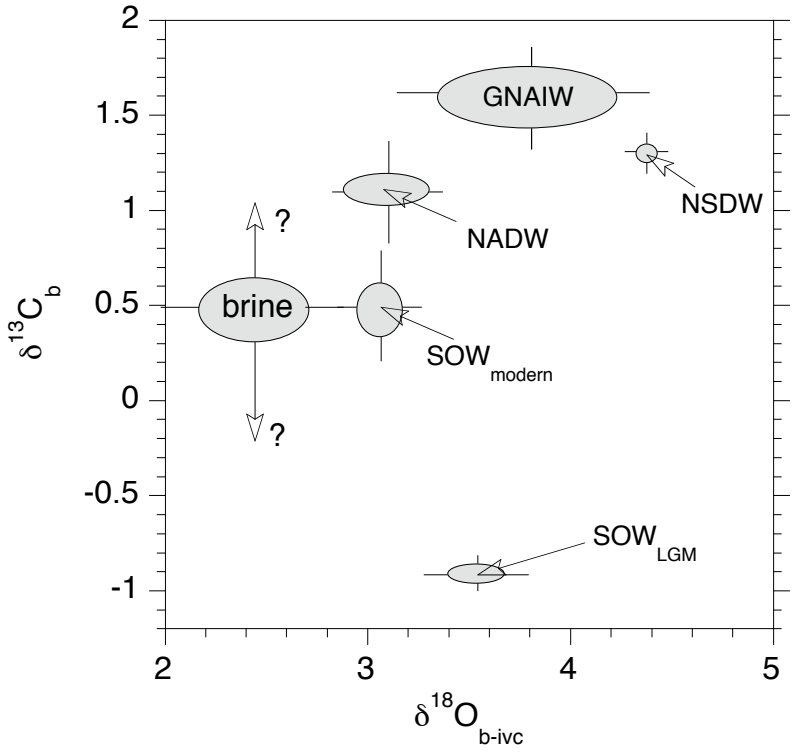
GNAIW
NSDW
NADW
?
brine
?
SOW modern
SOW LGM
2
1.5
1
0.5
0
-0.5
-1
2
3
4
5
δ13Cb
δ18Ob-ivc

Figure 4

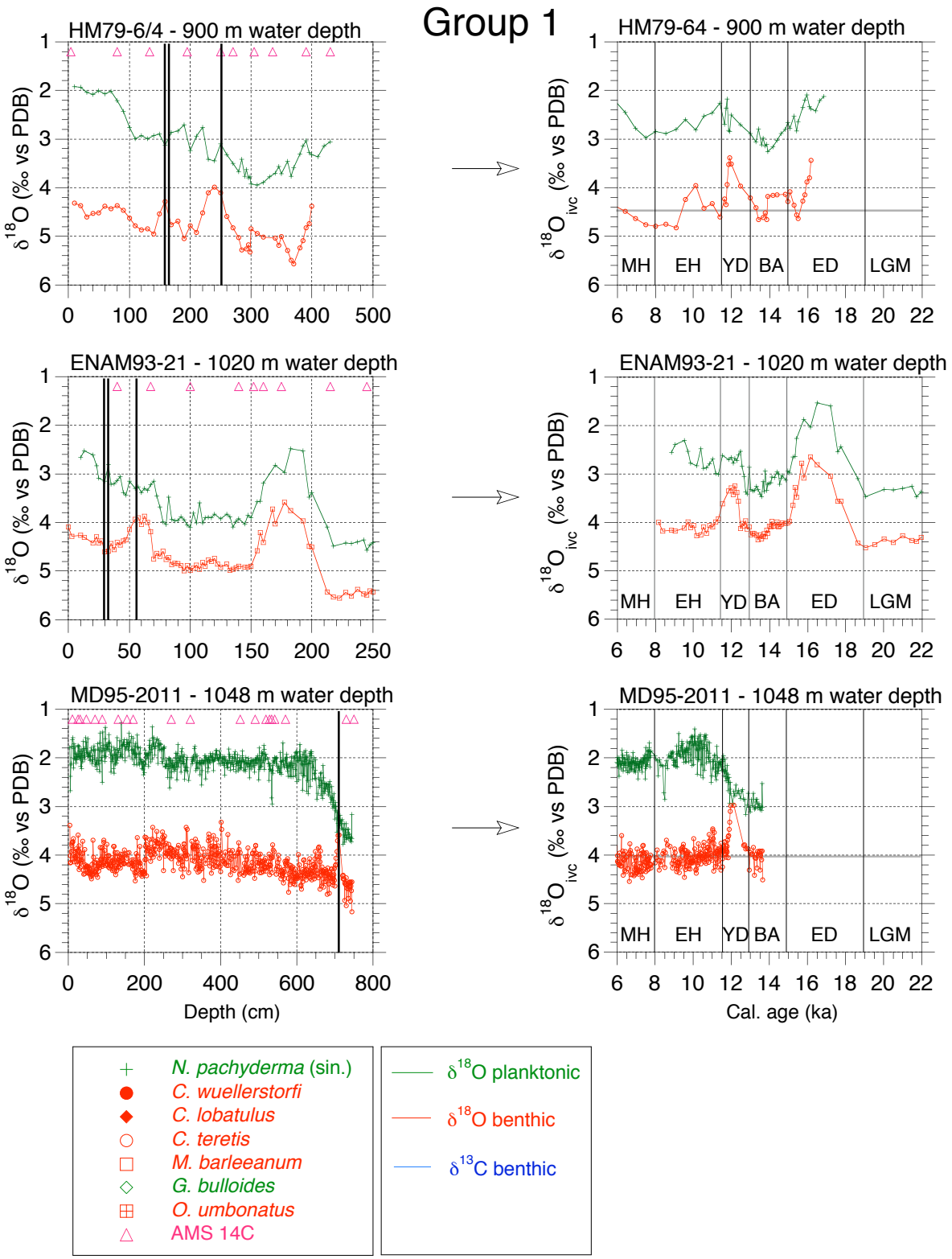

Figure 5 - page 1

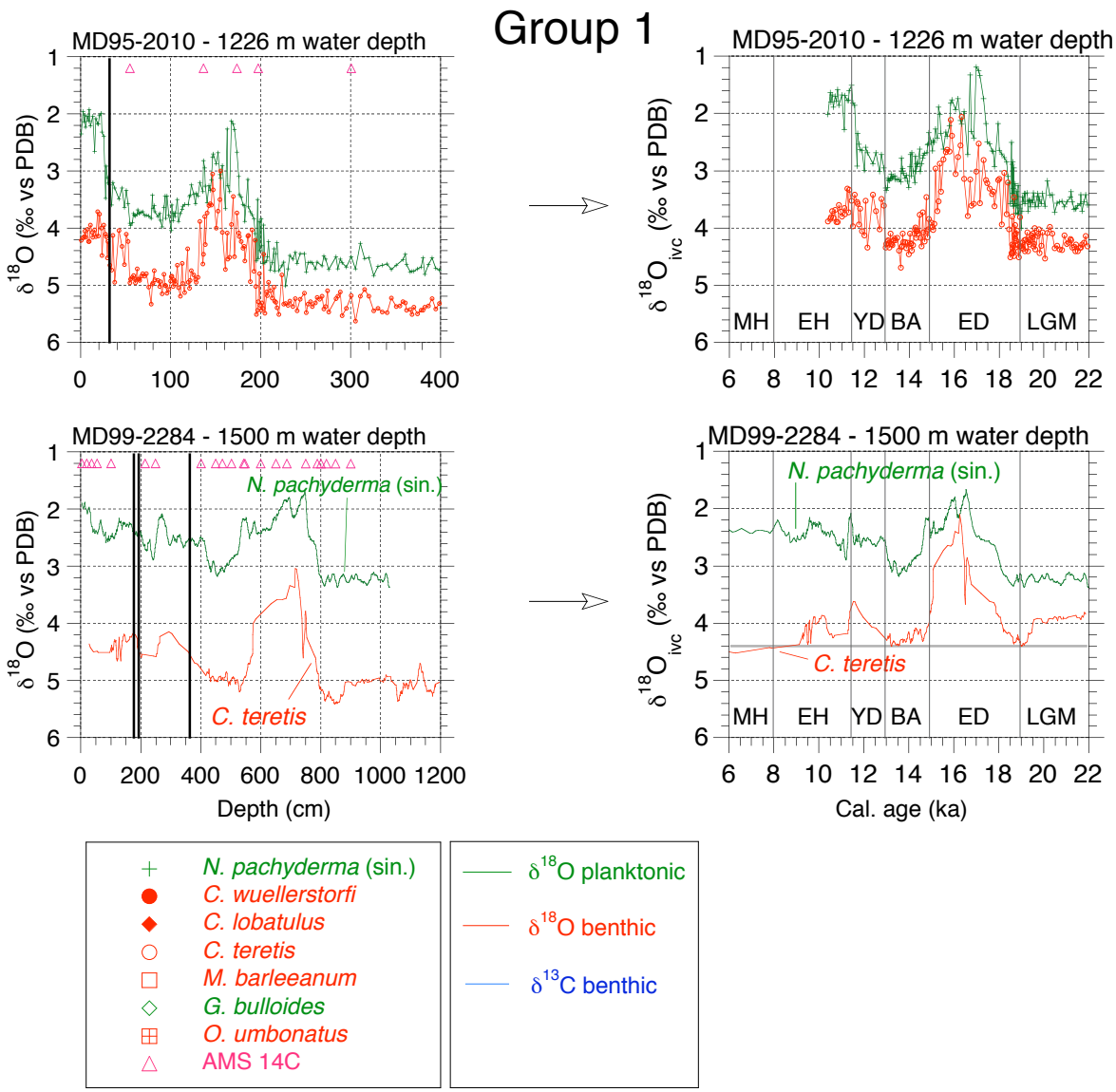

Figure 5 - page 2

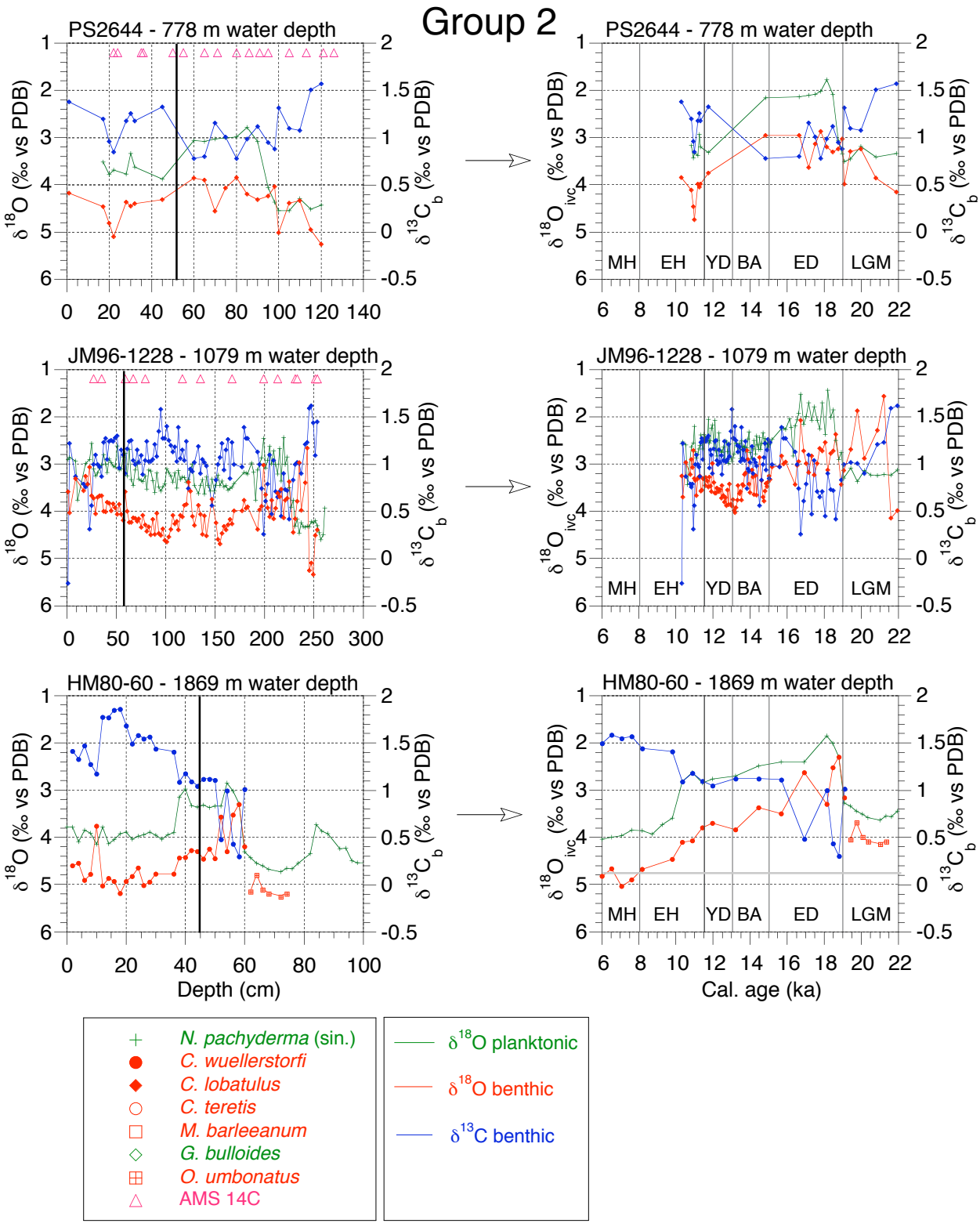

Figure 5 - page 3

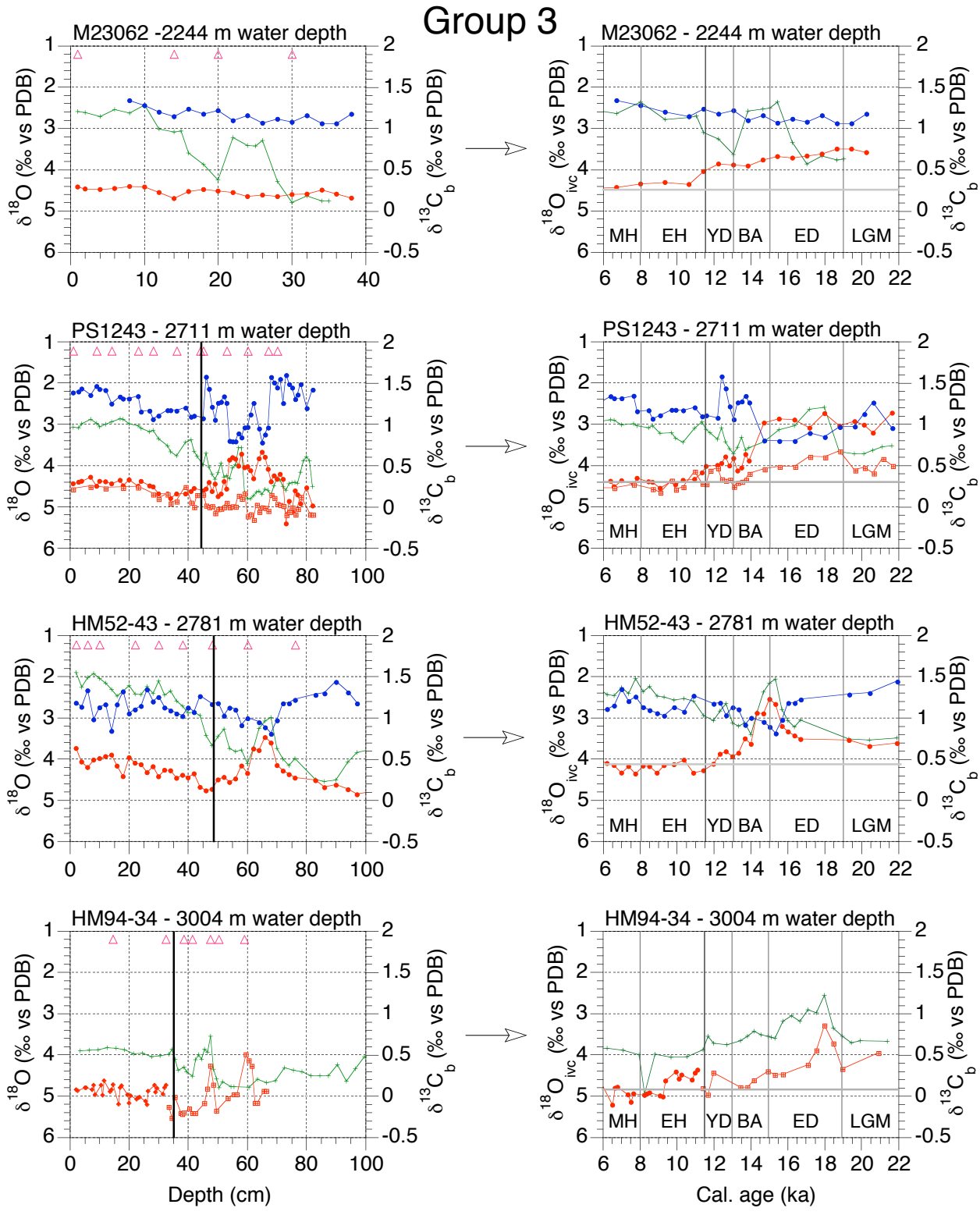

Figure 5 - page 4

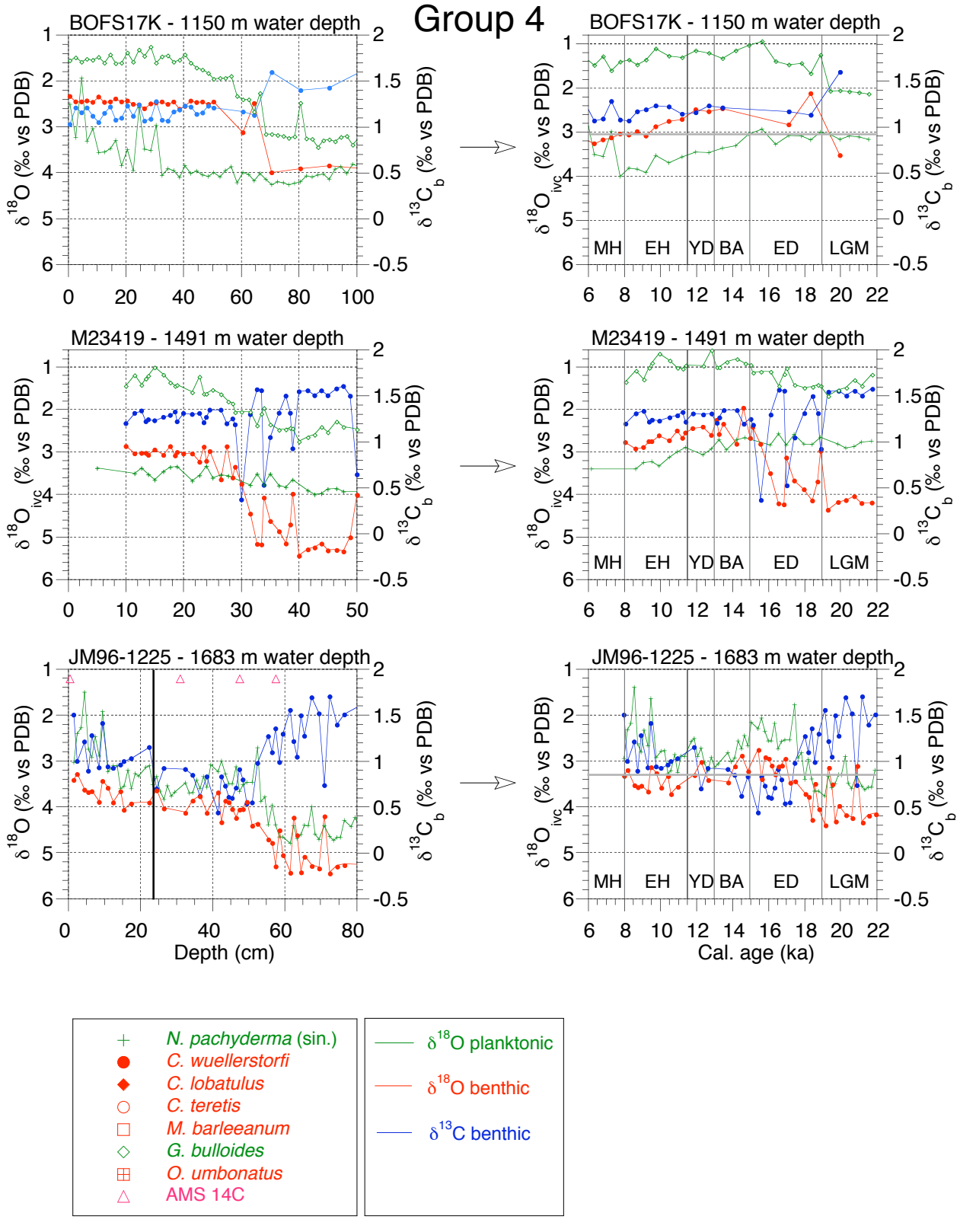

Figure 5 - page 5

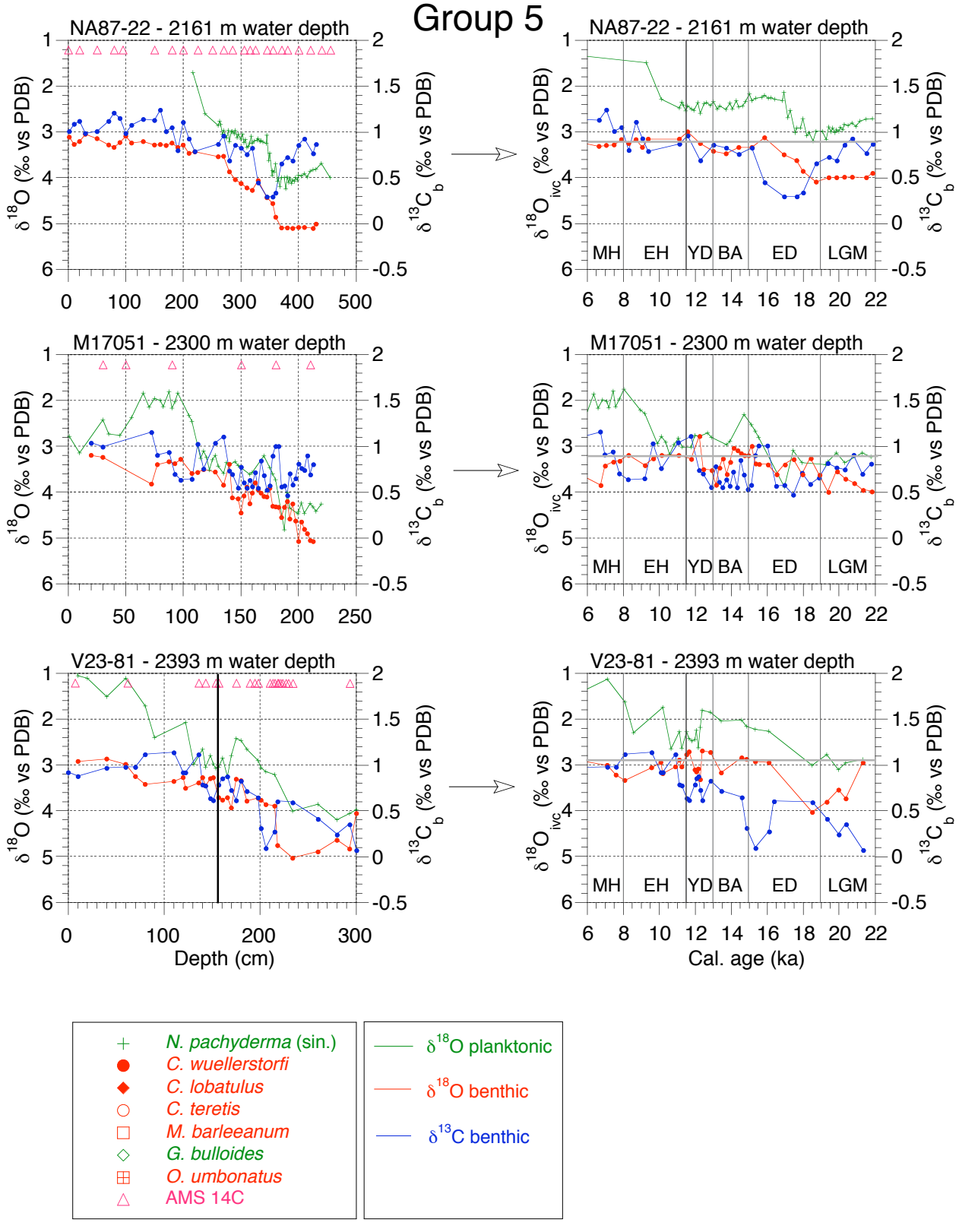
Group 5
NA87-22 - 2161 m water depth
M17051 - 2300 m water depth
V23-81 - 2393 m water depth
δ18O (‰ vs PDB)
δ13Cb (‰ vs PDB)
δ18Oivc (‰ vs PDB)
MH
EH
YD
BA
ED
LGM
Depth (cm)
Cal. age (ka)
N. pachyderma (sin.)
C. wuellerstorfi
C. lobatulus
C. teretis
M. barleeanum
G. bulloides
O. umbonatus
AMS 14C
δ18O planktonic
δ18O benthic
δ13C benthic

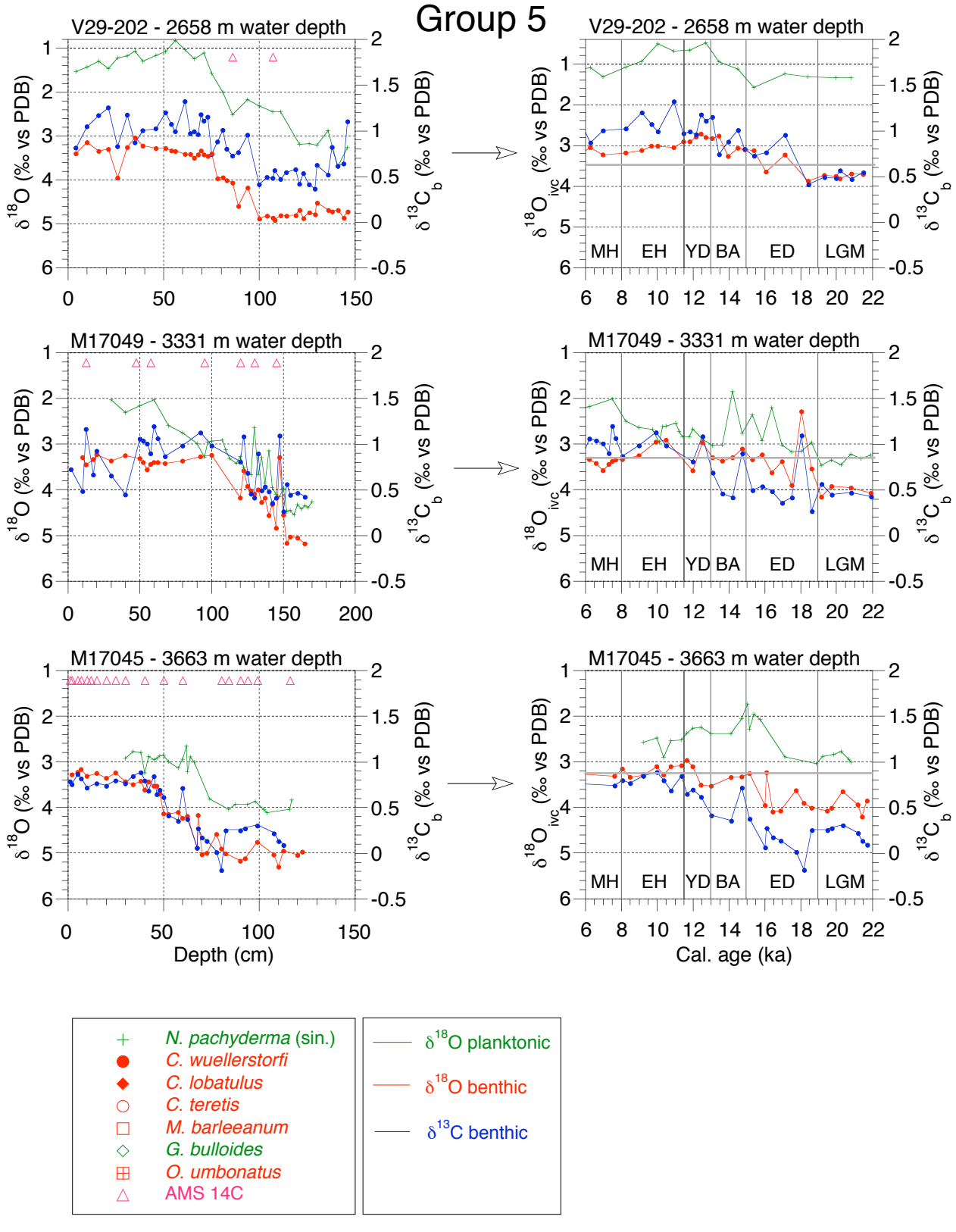
Group 5
V29-202 - 2658 m water depth
M17049 - 3331 m water depth
M17045 - 3663 m water depth
δ18O (‰ vs PDB)
δ13Cb (‰ vs PDB)
δ18Oivc (‰ vs PDB)
Depth (cm)
Cal. age (ka)
MH
EH
YD
BA
ED
LGM
N. pachyderma (sin.)
C. wuellerstorfi
C. lobatulus
C. teretis
M. barleeanum
G. bulloides
O. umbonatus
AMS 14C
δ18O planktonic
δ18O benthic
δ13C benthic

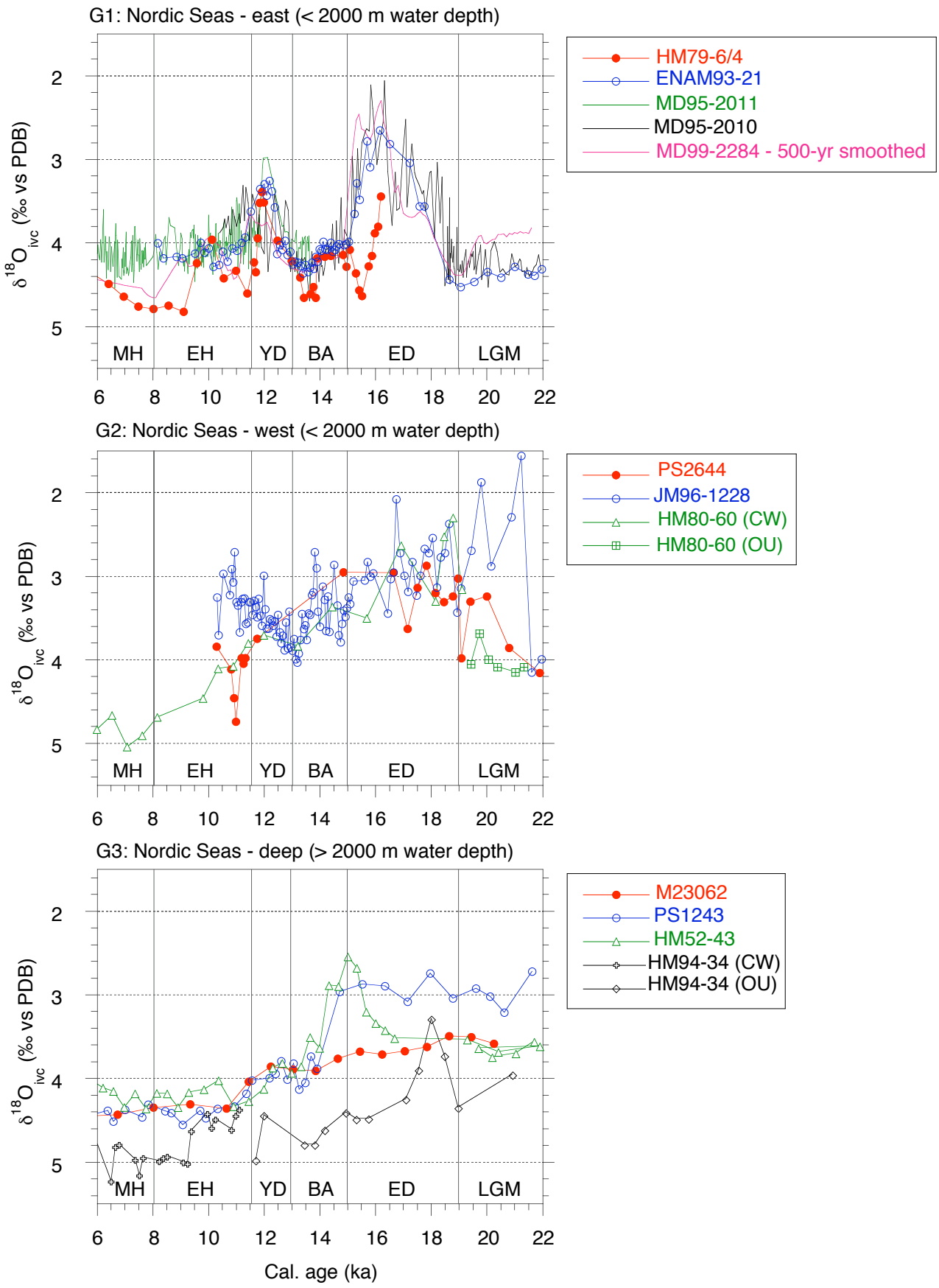

Figure 6 - page 1

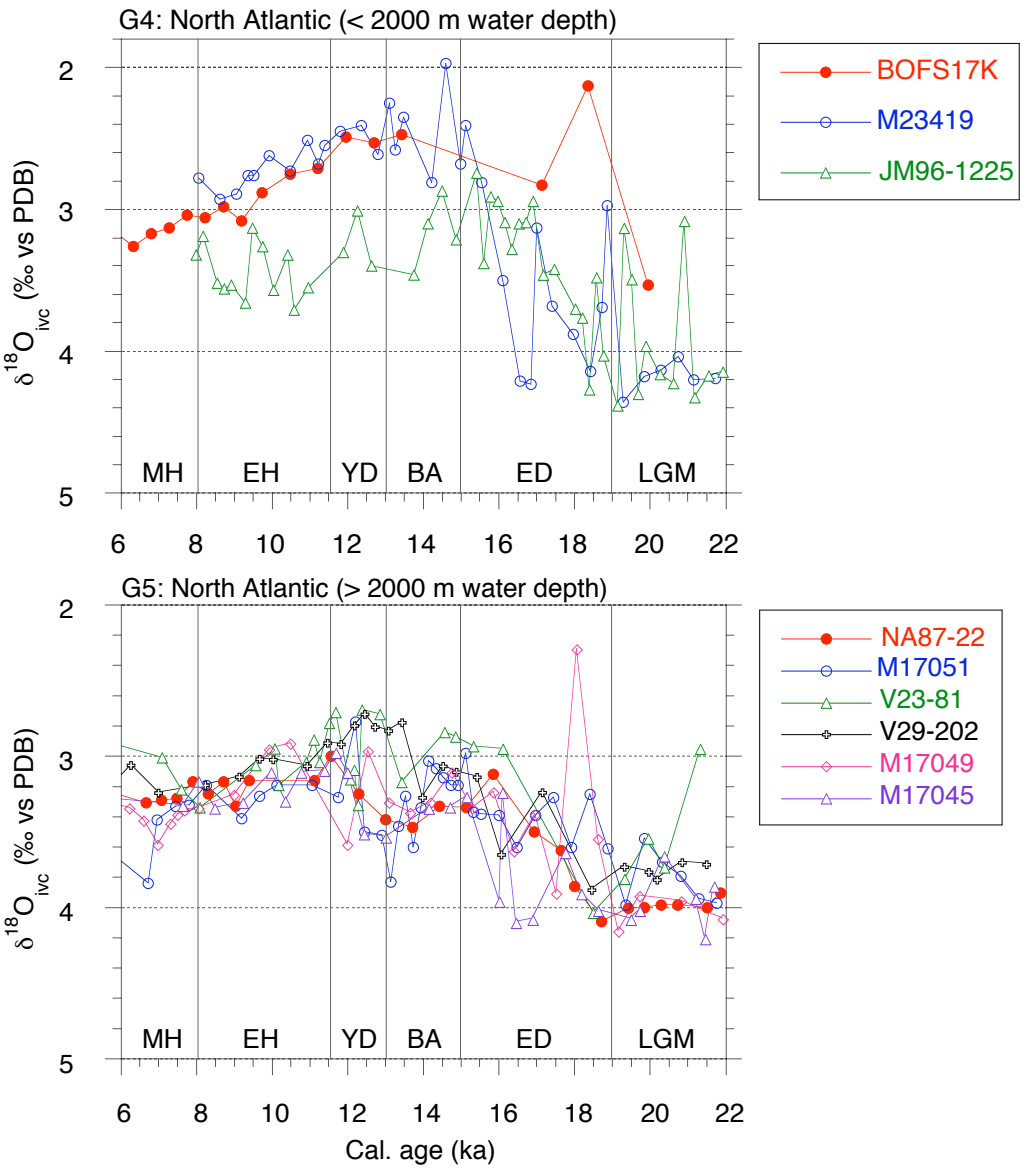

Figure 6 - page 2

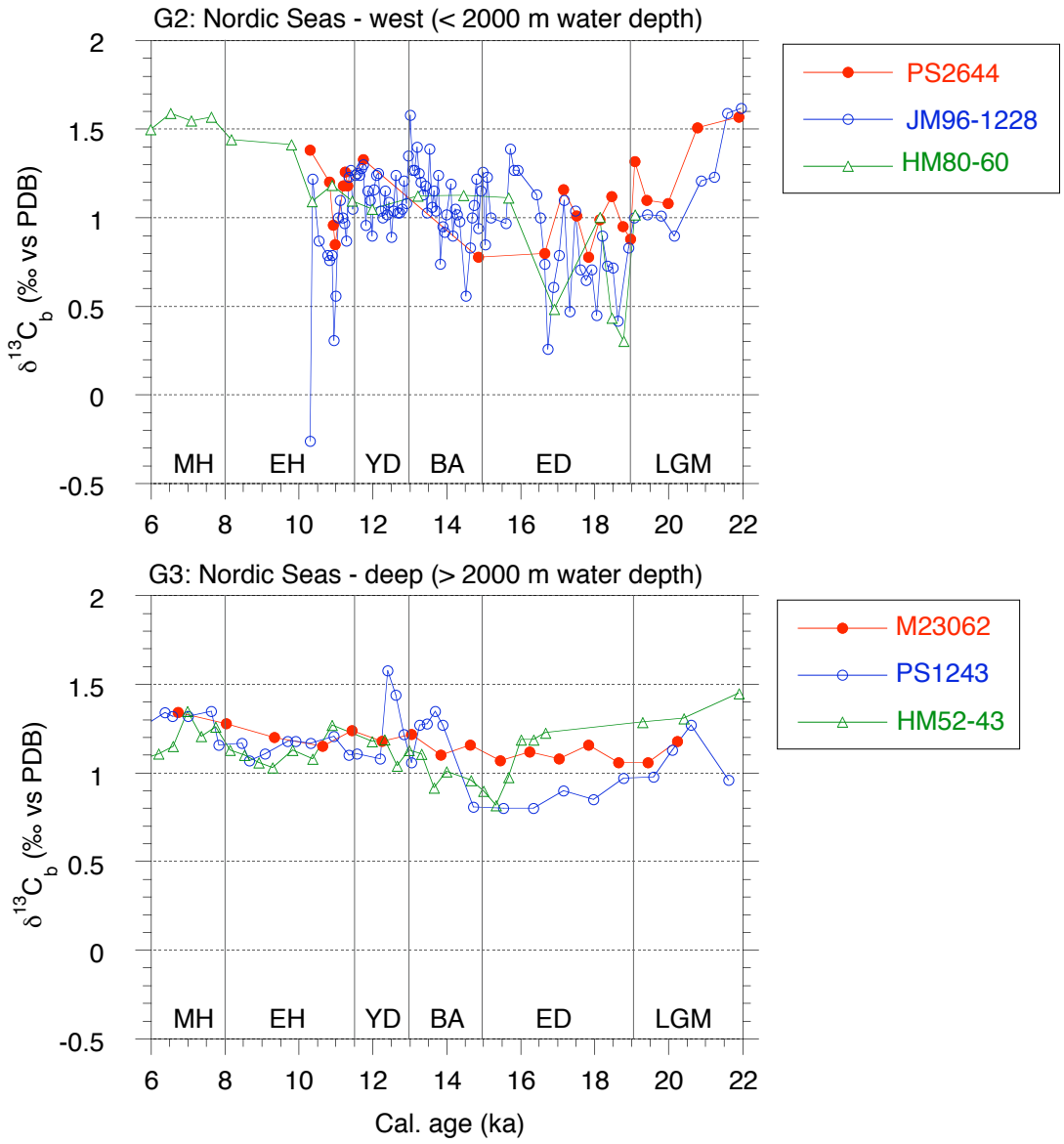

Figure 7 - page 1

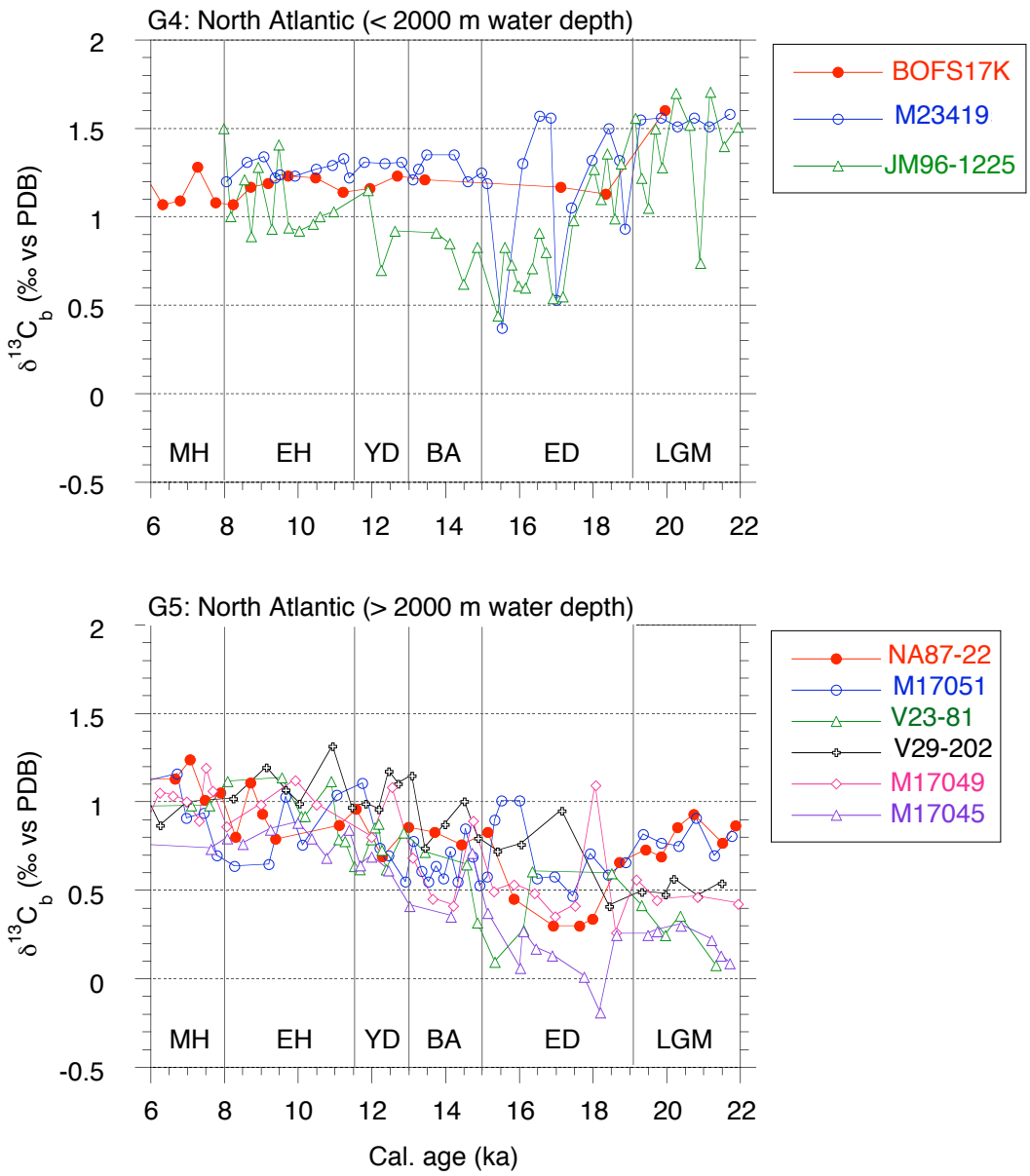

Figure 7 - page 2